

## Accepted Manuscript

### Arylamino Methylene Bisphosphonate Derivatives As Bone Seeking Matrix Metalloproteinase Inhibitors

Marilena Tauro, Antonio Laghezza, Fulvio Loiodice, Mariangela Agamennone, Cristina Campestre, Paolo Tortorella

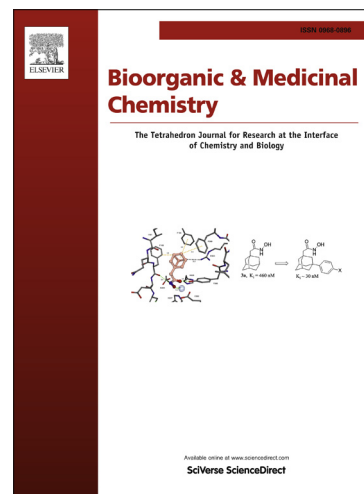
PII: S0968-0896(13)00757-8  
DOI: <http://dx.doi.org/10.1016/j.bmc.2013.08.054>  
Reference: BMC 11070

To appear in: *Bioorganic & Medicinal Chemistry*

Received Date: 28 March 2013  
Revised Date: 29 July 2013  
Accepted Date: 23 August 2013

Please cite this article as: Tauro, M., Laghezza, A., Loiodice, F., Agamennone, M., Campestre, C., Tortorella, P., Arylamino Methylene Bisphosphonate Derivatives As Bone Seeking Matrix Metalloproteinase Inhibitors, *Bioorganic & Medicinal Chemistry* (2013), doi: <http://dx.doi.org/10.1016/j.bmc.2013.08.054>

This is a PDF file of an unedited manuscript that has been accepted for publication. As a service to our customers we are providing this early version of the manuscript. The manuscript will undergo copyediting, typesetting, and review of the resulting proof before it is published in its final form. Please note that during the production process errors may be discovered which could affect the content, and all legal disclaimers that apply to the journal pertain.



**ARYLAMINO METHYLENE BISPHOSPHONATE DERIVATIVES AS BONE SEEKING MATRIX METALLOPROTEINASE INHIBITORS**

Marilena Tauro<sup>a</sup>, Antonio Laghezza<sup>a</sup>, Fulvio Loiodice<sup>a</sup>, Mariangela Agamennone<sup>b</sup>, Cristina Campestre<sup>b</sup>, Paolo Tortorella<sup>a\*</sup>

<sup>a</sup>Dipartimento di Farmacia-Scienze del Farmaco, Università degli Studi "Aldo Moro" di Bari, Via Orabona 4, 70126 Bari (Italy). Fax +39 080 5442231.

<sup>b</sup>Dipartimento di Farmacia, Università "G. d'Annunzio" Chieti, Via dei Vestini 31, 66013 Chieti (Italy)

\* Corresponding author: Dipartimento di Farmacia-Scienze del Farmaco, Università degli Studi "Aldo Moro" di Bari, Via Orabona 4, 70126 Bari (Italy). Tel. +39 0805442735, Fax +39 0805442231. E-mail: [paolo.tortorella@uniba.it](mailto:paolo.tortorella@uniba.it)

**Abstract**

The complexity of matrix metalloproteinases inhibitors (MMPIs) design derives from the difficulty in carefully addressing their inhibitory activity towards the MMP isoforms involved in many pathological conditions. In particular, specific metalloproteinases, such as MMP-2 and MMP-9, are key regulators of the "vicious cycle" occurring between tumor metastases growth and bone remodeling. In an attempt to devise new approaches to selective inhibitor derivatives, we describe novel bisphosphonate bone seeking MMP inhibitors (BP-MMPIs), capable to be selectively targeted and to overcome undesired side effects of broad spectrum MMPIs.

In vitro activity (IC<sub>50</sub> values) for each inhibitor was determined against MMP-2, -8, -9 and -14, because of their relevant role in skeletal development and renewal. The results show that BP-MMPIs reached IC<sub>50</sub> values of enzymatic inhibition in the low micromolar range. Computational studies, used to rationalize some trends in the observed inhibitory profiles, suggest a possible differential binding mode in MMP-2 that explains the selective inhibition of this isoform.

In addition, survival assay was conducted on J774 cell line, a well known model system used to evaluate the structure–activity relationship of BPs for inhibiting bone resorption. The resulting data, confirming the specific activity of BP-MMPIs, and their additional proved propensity to bind hydroxyapatite powder in vitro, suggest a potential use of BP-MMPIs in skeletal malignancies.

**1. Introduction**

Bone is a frequent site of metastases for several cancers. In 2012, the American Cancer Society estimated that approximately 68,000 men and women will succumb to prostate and breast cancers (www.cancer.org Cancer Facts and Figures American Cancer Society 2012) and studies predicted that 80-90% of these patients will have evidence of bone metastases at the time of their death. Bone metastases induce skeletal related events (SRE), including hypercalcemia and spontaneous pathologic bone fracture that can cause intense pain and greatly impact the patient's quality of life.[1, 2] The bone microenvironment provides a fertile soil for the growth and expansions of tumor cells, altering the physiological remodeling process.

Bone remodeling is a delicate balance between bone matrix synthesizing osteoblasts and bone resorbing osteoclasts activities. Active bone metastases typically subvert this process to generate lesions that include extensive areas of pathological osteogenesis and osteolysis.[3] The resultant increase in bone matrix remodeling enhances cytokine/growth factors bioavailability thus creating a vicious cycle that stimulates tumor assessment and progression at the bone site.[4]

Recent studies have identified matrix metalloproteinases (MMPs) as key regulators of this cycle, and pre-clinical experiments have reported the efficacy of broad spectrum metalloproteinase inhibitors (MMPIs) in preventing the skeletal related events secondary to prostate and breast tumors evolution.[4, 5] MMP-2 and -9 play a key role in the progression of the vicious cycle, while the first one derives from osteoblast, the second one is secreted by osteoblasts, osteoclasts and tumor cells. In this way they considerably contribute to promote tumor survival at the mineral surface of the host microenvironment, by regulating the bioavailability of TGF- $\beta$ , PTHrP and RANKL that are traditionally associated with driving that vicious cycle.[4]

Besides, remodeling of the bone matrix is required to accommodate the expansion of metastases and unsurprisingly, matrix metalloproteinases (MMPs) are over-expressed at the tumor-bone interface due to their central role in the processing of type I collagen-rich osteoid and other bone matrix components.[5, 6] MMPs also hydrolyze a number of other proteinases and some of them are involved in invasion and angiogenic mechanisms. Accordingly, while the selective inhibition of a limited set of MMPs is of relevant importance at the early stages of the disease, broad-spectrum inhibitors allow to intervene during the progression of the pathology. MMPIs are able to disrupt the vicious cycle occurring in the spread of tumor cells to bone; their possible therapeutic utility, however, is limited by the typical side effects of broad spectrum activity. Nonetheless, these adverse effects could be reduced by using molecules able to selectively target a specific tissue as proposed for bisphosphonates whose bone accumulation is well known.[7] It is clear that these compounds could represent an additional treatment strategy for patients with debilitating bone metastases.

Since MMPs belong to the family of zinc-containing enzymes, they are characterized by the presence of a zinc ion at the active site, responsible for the amide bond hydrolysis. An effective MMPI should satisfy the following requirements: (1) the presence of a functional group able to bind the catalytic  $Zn^{2+}$  ion of the enzyme; (2) at least one functional group capable to form hydrogen bonds with the enzyme backbone; (3) one or more moieties that can have effective van der Waals interactions with the enzyme subsites.

Hydroxamate has been considered for a long time the most potent zinc binding group (ZBG), able to work as a bidentate ligand with an optimum distance (1.9 – 3.3 Å) between the oxygen atoms and the active site  $Zn^{2+}$  ion.[8, 9] Although pharmaceutical companies have developed very potent hydroxamic inhibitors in the last 25 years, still no MMPIs are present in the market as anticancer agents. The reasons for the failure of clinical trials are multifold, mainly correlated with their relatively low selectivity, pharmacokinetics and toxicological problems.[10, 11]

We have been studying non-hydroxamic MMPIs for a long time.[12-19] In a recent paper we reported a series of inhibitors characterized by a bisphosphonic core (BP-MMPIs), a well known bone seeking moiety, as ZBG.[20] The benefits deriving from the introduction of this ZBG are twofold. Firstly, it realizes an efficient interaction with the catalytic zinc ion, inhibiting the proteolytic activity of matrix

metalloproteinases involved in several pathological conditions. Secondly, the molecules are more effective towards MMPs involved in the vicious cycle, since bone targeting concentrates the pharmacological agents at the desired active site allowing a more potent effect without increasing the administered dose.[7]

The present work stems from the demonstrated MMPs inhibitory activity of some bisphosphonic drugs already clinically used in osteoporosis disease.[20] In particular tiludronate and zoledronate (Fig.1) have shown a very interesting activity against MMP-2 and MMP-8, but none of them realized a satisfactory activity against MMP-9, a fundamental target of the vicious cycle. This prompted us to develop a new series of analogues, capable of selective bone targeting and disrupting the vicious cycle of bone tumor growth through MMP-2 and MMP-9 inhibition.

In this context, we report herein the synthesis of arylamino methylene bisphosphonates (Fig.1) and their biological evaluation against various MMPs involved in skeletal formation (Table 1).

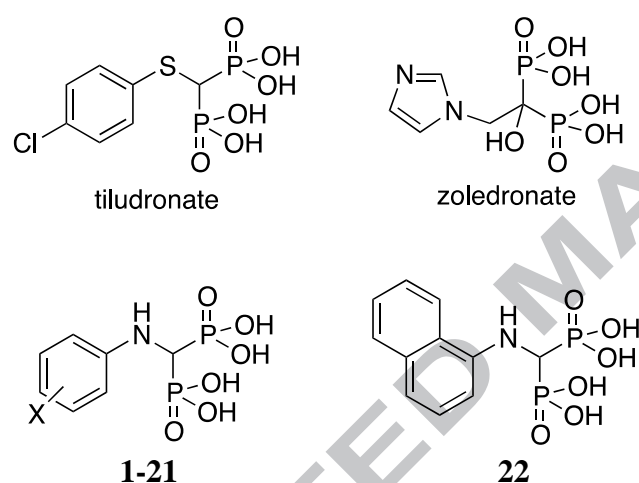


**Figure 1.** Chemical structures of bisphosphonate derivatives. Substituents X in **1-21** are presented in Table 1

In order to evaluate the mineral bond affinity of the synthesized compounds, we decided to assess their binding to hydroxyapatite (HAP), the main constituent of bone. This value, in fact, is considered as a measurement of the selective targeting effect of bisphosphonic moiety towards the bone matrix surface.[21-23] We also evaluated the effect of these compounds directly on J774 vitality as indicative of an osteoclast activity. Promising results were expected based on the recent paper about tetraphenyl(phenylamino)methylene bisphosphonates showing remarkable decrease in osteoclastic bone resorption compared to the commercial drug alendronate.[24]

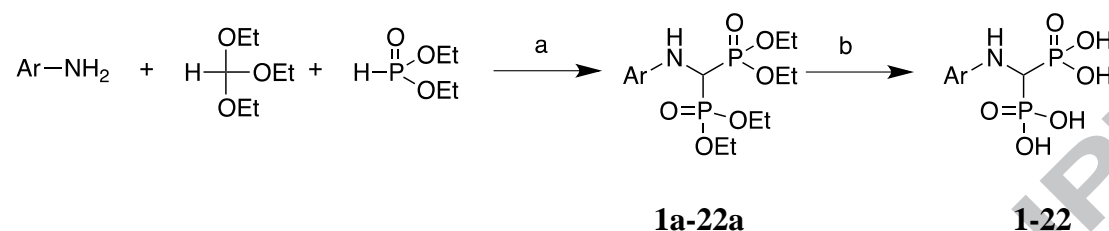
## 2. Results and discussion

### 2.1 Chemistry

Reference compounds tiludronate and zoledronate were prepared as previously reported.[20]

Arylamino methylene bisphosphonic acids **1-22** were prepared as reported in Scheme 1. The one pot condensation of the suitable arylamines (1eq.) with diethyl phosphite

(1.2 eq.) in the presence of triethyl orthoformate (3 eq.), followed by de-alkylation with trimethylsilyl bromide in anhydrous acetonitrile of the corresponding tetraethyl ester intermediates **1a-22a** led to the final acids **1-22**.



**Scheme 1.** a) 160°C, 3-4h; b) (CH<sub>3</sub>)<sub>3</sub>SiBr, CH<sub>3</sub>CN, 48-72h, MeOH.

## 2.2 MMP activity

In the first part of this work we decided to use tiludronate as a template and to modify its structure by replacement of sulfur atom with an isosteric amine function and introduction of different substituents on the aromatic ring. These substituents were selected in order to explore the role of lipophilic ( $\pi$  of Hansch), electronic ( $\sigma$  of Hammett) and steric ( $E_s$  of Taft) parameters [25] on MMP inhibiting activity. With this aim, a set of bisphosphonates have been synthesized and tested against MMP-2, -8, -9 and -14. These particular MMP isoforms were selected due to their recognized critical role in skeletal development and remodeling and their function in the progression of tumor metastases.

**Table 1.** MMP inhibition activity (IC<sub>50</sub>  $\mu$ M)

Entry	X	MMP-2	MMP-8	MMP-9	MMP-14
<i>tiludronate</i>		7.2±0.5	32±3	>100	30.5±1.6
<i>zoledronate</i>		7.0±1.3	17.6±4.6	52±6	12.6±0.1
<b>1</b>	H	>100	>100	>100	>100
<b>2</b>	4-F	28.2±1.3	>100	>100	>100
<b>3</b>	4-Cl	>100	>100	>100	>100
<b>4</b>	4-Br	6±3	2.4±0.4	30±7	3.9±1.7
<b>5</b>	4-NO <sub>2</sub>	20±10	15±2	20±6	26±5
<b>6</b>	4-CH <sub>3</sub>	>100	36±4	>100	>100
<b>7</b>	4-CF <sub>3</sub>	15±4	>100	>100	>100
<b>8</b>	4-CN	36±4	>100	>100	>100
<b>9</b>	4-OH	6.6±0.7	>100	>100	>100
<b>10</b>	3-NO <sub>2</sub>	15.5±0.5	>100	>100	>100
<b>11</b>	3-CF <sub>3</sub>	20.8±1.2	>100	>100	>100
<b>12</b>	3-F	42±8	>100	>100	>100
<b>13</b>	3-Br	37.4±2.1	>100	>100	>100
<b>14</b>	3,4-Cl	>100	25.5±0.4	>100	20±5
<b>15</b>	3-NO <sub>2</sub> , 4-F	25±3	>100	>100	>100

<b>16</b>	2,4-Cl	>100	>100	>100	>100
<b>17</b>	4-Ph	>100	30±5	>100	33.5±2.1
<b>18</b>	4-Ph-O	2.8±0.4	44±4	>100	43±14
<b>19</b>	4-(4-Cl-PhO)	2.1±0.5	39.9±0.2	55±18	76±7
<b>20</b>	4-(4-Br-PhO)	2.8±0.1	43±3	87±4	49.5±2.3
<b>21</b>	3-Ph	>100	52±10	>100	40±4
<b>22</b>		6.4±1.4	61±20	6.0±1.2	69±8

Although the replacement of sulfur atom of tiludronate with an amine group is not functional to the improvement of the MMP inhibitory activity profile (compounds **3** and **1**), the specific MMPs effectiveness can be restored by introduction of different groups on the aromatic ring of **1**. The obtained results show, therefore, that the interactions at the different enzymatic active sites can be modulated by a suitable regulation of lipophilic, electronic and steric effects.

Overall micromolar inhibition has been obtained; compound **4** shows the highest inhibitory activity towards MMP-8 and -14 ( $IC_{50}=2.4\mu M$  and  $3.9\mu M$ , respectively), whereas compounds **19** and **22** are, respectively, the most potent on MMP-2 and MMP-9, ( $IC_{50}=2.1\mu M$  and  $6.0\mu M$ ). These BPs exhibit an improved inhibition profile compared to tiludronate, confirming their promising capability to be more effective towards specific bone MMP contribution in the vicious cycle.

Notably, this series of BPs shows a quite peculiar selectivity profile, in particular towards MMP-2 (**2**, **7-13**, **15**, **18-20**). Activity on this isoform seems to be affected by the presence of electron withdrawing groups on the phenyl ring as well as by the increase of lipophilicity of substituents as shown by **18-20**.

Actually, the same behavior is also observed for the 4-hydroxy derivative **9**; in this case, however, the effect could be ascribed to the predicted capability to form additional H bonds with amino acid residues in S1' pocket.

In contrast, the introduction of an electron donor substituent, as in the case of compound **6**, decreases the activity on all tested MMPs, even if a residual activity on MMP-8 still remains.

Interestingly, the substitution of the flexible phenoxybenzene substituent (**18-20**) with the more rigid biphenyl moiety (**17** and **21**) seems to reduce the activity against MMP-2.

A particular behavior is shown from the substitution with chlorine. The presence of this halogen in 4 or 2,4 positions (**3**, **16**) provides compounds devoid of any MMP enzymatic inhibition; however, moving chlorine from 2 to 3 position (**14**), a shift of selective inhibitory activity from MMP-2, as shown by all 3-substituted analogues, to MMP-8 and -14 occurs.

In summary, the newly synthesized bisphosphonic molecules show low-micromolar  $IC_{50}$  values towards MMP-2, whose pivotal role is already proven in the progression of cancer bone metastases. However, the broad spectrum activity of compounds **4** and **5** on all the tested MMP isoforms represents an additional benefit because of the key role of MMP-2, -8, -9 and -14 in the physiopathology of skeletal renewal.

Furthermore compound **22** shows comparable activities on both MMP-2 and -9, and it represents the most promising BP-MMPI candidate for disrupting the vicious cycle.

Worthy of note is the effectiveness of compound **22** towards MMP-9, whose inhibition always encounters some difficulties, as previously observed for sulfonamide BPs,[20] for tiludronate and zoledronate.

In order to rationalize the inhibition data and in particular to explain the different activity profiles among tested MMPs, all ligands were docked into the X-ray structure of MMP-2, -8, -9 and -14 applying a flexible docking approach, using Glide. Best poses were subsequently minimized exploiting the Embrace module of MacroModel to improve the positioning of ligands and calculate the different contributions to the binding energy (obtained energies are reported in Tables 6-9 of the Supporting Information).

The predicted binding mode of all active ligands towards MMP-8, -9 and -14, and compounds **4**, **5**, **9**, **18-20** and **22** to MMP-2, is well conserved: they occupy the S1' site, providing the  $\pi$ - $\pi$  stacking interaction with the His201 side chain (MMP-2 numbering). The bisphosphonate function is not able to chelate the zinc ion, therefore just one phosphonic group coordinates the  $Zn^{2+}$ , while the other one forms two H-bonds with the NH of Leu164 and Ala165 or alternatively with Pro221 CO, similarly to what observed for sulfonamide BP.[20] In Figure 2 the conserved binding mode of broad spectrum inhibitors **4** and **5** into the MMP-2 active site is represented.

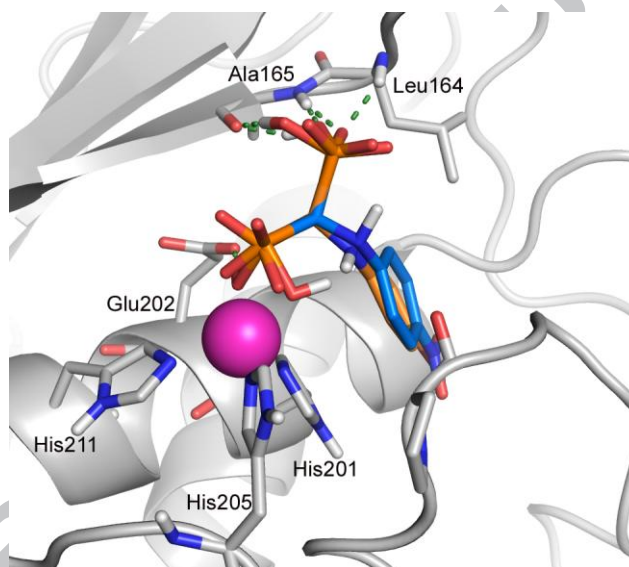


**Figure 2.** Superimposition of docked poses of compounds **4** (orange C atoms) and **5** (blue C atoms) into MMP-2. MMP-2 structure is represented as grey cartoon. Zinc ion is depicted as a purple sphere. Ligands and most relevant receptor residues are represented as sticks. H-bonds are represented as green dashed lines.

MMP-9 inhibition by compound **22** can be due to a favorable positioning of the ligand that forms hydrophobic interactions in the proximal region of the S1' site with Tyr423, Leu188, Val398, Leu418 and provides an extended  $\pi$ - $\pi$  stacking interaction with His401; moreover, the amino methylene-bisphosphonate group forms a H-bond network with Leu188 and Pro421 (Fig. 3).

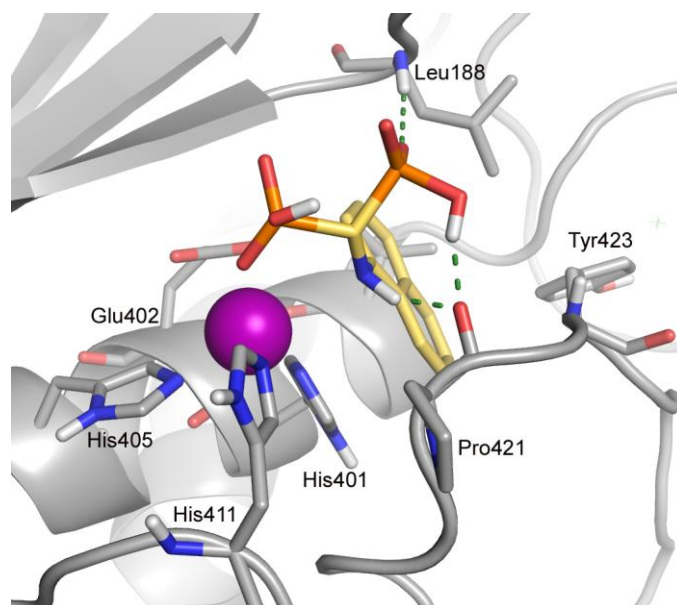


**Figure 3.** Docked pose of compound **22** into MMP-9. MMP-9 structure is represented as dark grey cartoon. Zinc ion is depicted as a purple sphere. Ligands and most relevant receptor residues are represented as sticks. H-bonds are represented as green dashed lines.

Activity data on MMP-2 indicate a dual trend: larger and more hydrophobic compounds and smaller and hydrophilic ligands are both active. The first behavior is in line with the results previously discussed for the other MMPs, while docking results reveal that smaller and more hydrophilic ligands bind MMP-2 with the bisphosphonate function chelating the zinc ion, and the aromatic ring occupying the S1 and S3 site, instead of the deep S1' site (Fig. 4). The only exception is represented by compound **9** that, as already stated, binds the S1' site. This result is quite surprising as all MMPs share a very conserved binding mode and the hydrophobic contact in the S1' site is widely considered as the leading interaction for MMPs inhibition.

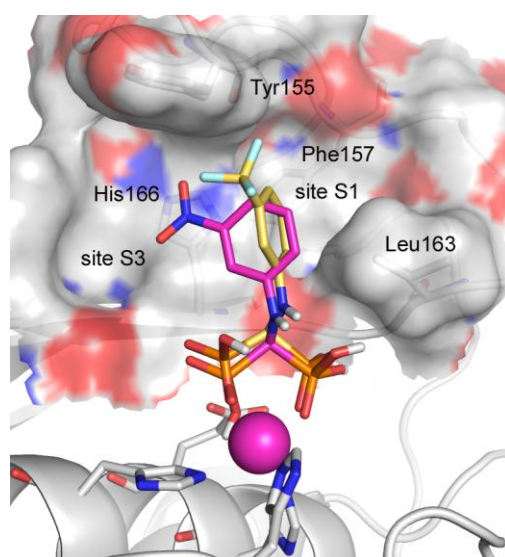


**Figure 4.** Superimposition of docked poses of compounds **10** (magenta C atoms) and **11** (yellow C atoms) into MMP-2.

MMP-2 structure is represented as grey cartoon. Zinc ion is depicted as a purple sphere and ligands as sticks. H-bonds are represented as green dashed lines. For clarity the molecular surface of S1 and S3 sites is shown.

Analysis of the binding poses shows that small compounds positioning in the S1 and S3 site is allowed by favorable interactions with Tyr155, Leu163, His166 and Phe157 residues. The different behavior of inhibitors towards MMP-2 with respect to MMP-8 and -14 can be at least partially attributed to the presence of Ser151 and Thr190 instead of Tyr155 in the S1 site of MMP-8 and MMP-14 respectively, that form much more solvent exposed S1 site. The S1 site of MMP-9 is much smaller and does not allow the binding of these ligands.

Targeting properties of the synthesized BPs at the bone site were investigated directly on hydroxyapatite powder (HAP), in order to predict their possible *in vivo* interaction. Among the different analytic techniques already described in the literature, such as HPLC [22, 26] or NMR [23] determinations, we decided to quantify relative binding affinity of this new set of bisphosphonates to hydroxyapatite through UV spectrophotometry technique.[27] This sensitive method, in fact, easily allows to detect and compare BPs affinity with that of tiludronate as shown in Table 2. We performed the experiment by adding hydroxyapatite powder to each BP solution and monitoring the residual amount of free compound remaining in solution by measuring its absorbance at the suitable wavelength.

**Table 2.** *In vitro* HAP binding affinity

<b>Entry</b>	<b>% adsorbed</b>
tiludronate	51.5±2.1
<b>1</b>	58±5
<b>2</b>	61.2±0.1
<b>3</b>	64.2±0.6
<b>4</b>	49±4
<b>5</b>	76.0±1.8
<b>6</b>	23.9±0.3
<b>7</b>	42.5±0.1
<b>8</b>	76.0±0.6
<b>9</b>	88.4±0.1
<b>10</b>	57.8±1.6
<b>11</b>	50.3±1.6
<b>12</b>	63.6±0.7
<b>13</b>	70.1±1.1
<b>14</b>	53.5±0.5
<b>15</b>	66.2±2.8
<b>16</b>	56.8±1.3
<b>17</b>	60±7
<b>18</b>	66.2±0.2
<b>19</b>	52.1±0.6

<b>20</b>	60.7±1.6
<b>21</b>	66.4±0.3
<b>22</b>	51.6±0.1

All the analyzed BPs show similar binding affinity to HAP in comparison with the already clinically used tiludronate and, as a consequence, probable same ability in bone targeting. However, compounds **5**, **8** and **9** stand out with their higher adsorption percentages to the mineral powder, reaching 76% and 88%, respectively. Our data suggest that only the introduction of the methyl substituent (entry **6**) significantly reduces the BP affinity for HAP.

To provide a more definite picture of bioavailability and drug-like properties of studied compounds, some physicochemical parameters were calculated (Table 3).

Table 3. Physicochemical properties calculated for tested compounds.

Name	mol MW	HBA <sup>a</sup>	HBD <sup>b</sup>	AlogP	RB <sup>c</sup>	PSA <sup>d</sup>	QLogSw <sup>e</sup>
Tiludronate	318.6	2	2	0.82	4	165.6	-1.02
Zoledronate	257.1	3	3	-2.61	4	170.2	1.21
1	267.1	2	3	-0.57	4	152.4	-0.82
2	285.1	2	3	-0.37	4	152.4	-1.16
3	301.6	2	3	0.09	4	152.4	-1.51
4	346.0	2	3	0.18	4	152.4	-1.61
5	312.1	2	3	-0.68	5	195.5	-0.89
6	281.1	2	3	-0.09	4	152.4	-1.27
7	335.1	2	3	0.37	5	152.4	-2.10
8	292.1	3	3	-0.69	4	176.2	-1.78
9	282.1	3	4	-0.84	4	172.6	-0.93
10	312.1	2	3	-0.68	5	195.5	-0.88
11	335.1	2	3	0.37	5	152.4	-2.18
12	285.1	2	3	-0.37	4	152.4	-1.16
13	346.0	2	3	0.18	4	152.4	-1.61
14	336.0	2	3	0.76	4	152.4	-2.08
15	330.1	2	3	-0.47	5	195.5	-1.11
16	336.0	2	3	0.76	4	152.4	-1.78
17	343.2	2	3	0.95	5	152.4	-2.54
18	359.2	3	3	0.99	6	161.6	-2.46
19	393.7	3	3	1.65	6	161.6	-3.18
20	438.1	3	3	1.74	6	161.6	-3.25
21	343.2	2	3	0.95	5	152.4	-2.51
22	317.2	2	3	0.34	4	152.4	-1.61

<sup>a</sup> Number of hydrogen-bond acceptor atoms; <sup>b</sup> Number of hydrogen-bond donor atoms; <sup>c</sup> Number of rotatable bonds; <sup>d</sup> Polar Surface Area; <sup>e</sup> Log of the calculated solubility in water.

It is worth noting that all compounds comply with the Lipinski's Rule of five, although recent research showed that the major disadvantage of the clinically utilized BPs is their poor oral adsorption from the gastrointestinal tract (typically <1% is adsorbed). [28] This behavior can be rationalized considering the high PSA value (Veber et al. define a maximum value of 140 Å<sup>2</sup> for drug-like compounds [29]), mainly due to the bisphosphonic moiety. This functional group, however, is responsible for the targeting on the bone tissue and therefore is mandatory for its activity. One strategy for improving oral absorption and permeability through cell

membrane of these types of molecules could be the development of more lipophilic derivatives. Our molecules **18-20** and **22** show the same HAP affinity but are more lipophilic than zoledronate or tiludronate as demonstrated by the AlogP values and, therefore, can be considered worth of following optimization.

### 2.3 Cell viability

Bisphosphonates bind avidly to exposed bone mineral around resorbing osteoclasts, resulting in very high levels of bisphosphonate in the resorption lacunae. At a cellular level, bisphosphonates are clearly targeting the osteoclasts and may inhibit their functions in several ways: 1) inhibition of osteoclast recruitment, 2) reduction of the osteoclast life span by direct apoptotic effect impairing osteoclast-mediated bone resorption, and 3) reduction of the tumor-associated osteolysis that is initiated by the development of skeletal metastases.[30]

We started analyzing the inhibitory effect of this new class of bisphosphonic compounds on the mouse macrophage cell line J774, that is a model system already used to screen BPs activity on osteoclast viability and functionality.[20, 31, 32] In order to evaluate the selective effect on J774 cell line, we treated also a non-myeloid derived cell type, via the human liver hepatocellular carcinoma cell line HepG2. The one way ANOVA analysis of obtained data (Fig. 5) shows a selective activity of these new BP-MMPIs against J774 cells. The observed lack of activity on HepG2 suggests that the effects of these BPs is not due to indiscriminate cytotoxicity. Though it is difficult to establish a correlation between the data obtained by cell-based assays and MMPs inhibition assay, compounds **9**, **18-20** showed interesting effects on both MMPs and J774 vitality; the two mechanisms could synergically act against the progression of bone loss associated with bone metastases.

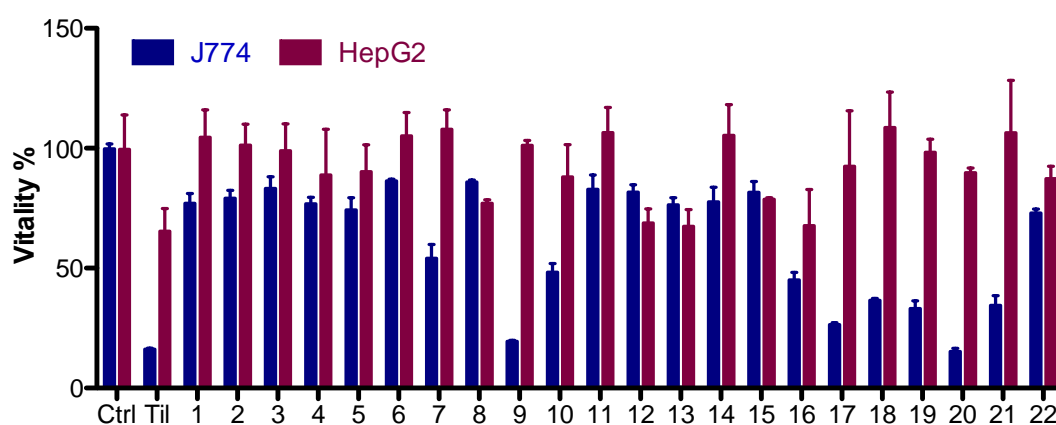


**Figure 5.** Graphical representation of cell % viability derived from MTT assay of compounds **1-22** in comparison with tiludronate at 100  $\mu$ M. The side-by-side comparison between BP-MMPIs effects on J774 mouse macrophage cell line and HepG2 hepatocellular carcinoma underlines the selectivity of action of BPs. Data processed by one-way analysis of variance (Bonferroni's Multiple Comparison Test) show that each BP-MMPI presents a statistical significance of  $P < 0.001$  from control.

### 3. Conclusions

A new series of bisphosphonates was synthesized and tested. A good effectiveness on MMP-2 was reached by compounds **4**, **9**, **18**, **19**, **20** and **22**, with the last one having the same IC<sub>50</sub> value on MMP-9. The activity on these two MMPs which have a key role in the vicious cycle occurring in bone formation metastatic process, combined with the selective inhibitory effects on J774 cells and the proven high affinity for HAP, allows to consider these BP-MMPIs as new promising agents for bone malignancy treatment.

## 4. Experimental section

### 4.1 Chemistry

Melting points were determined in open capillaries on a Gallenkamp electrothermal apparatus and are uncorrected. Mass spectra were recorded on a HP MS 6890–5973 MSD spectrometer, electron impact 70 eV, equipped with a HP ChemStation or with an Agilent LC-MS 1100 Series LC-MSD Trap System VL spectrometer, electrospray ionization (ESI). <sup>1</sup>H and <sup>31</sup>P NMR spectra were recorded using the suitable deuterated solvent on a Varian Mercury 300 NMR Spectrometer. Chemical shifts (δ) are expressed as parts per million (ppm) and the coupling constants (J) in Hertz (Hz). Microanalyses of solid compounds were carried out with a Eurovector Euro EA 3000 model analyzer; the analytical results are within ± 0.4% of theoretical values. Flash column chromatography was performed using Geduran silica gel 60 Å (45–63 μm). Chemicals were purchased from Aldrich Chemicals (Milan, Italy) and were used without any further purification.

UV quantification was effectuated with UV/Vis Spectrometer Perkin Elmer, Lambda Bio 20.

#### **Tetraethyl [(arylamino)methyl]-1,1-bisphosphonates. General procedure.**

Triethylorthoformate (1.2 mmol), diethyl phosphite (3 mmol) and the suitable aniline (1 mmol) were added in a 5 mL round bottom flask fitted with a distillation apparatus. The resulting mixture was heated at 160°C under argon atmosphere, until the evolution of EtOH was completed and the residue was dissolved in ethyl acetate. The solvent was distilled off affording a crude yellow oil, which was purified on a silica gel column using ethyl acetate as eluent. The titled compounds were obtained as white solids in 32-89% yield.

**Tetraethyl [(phenylamino)methyl]-1,1-bisphosphonate (1a).** 53% yield; <sup>1</sup>HNMR (CDCl<sub>3</sub>): δ 1.21-1.30 (m, 12H, CH<sub>3</sub>), 4.07-4.27 (m, 10H, CH<sub>2</sub>, CH, NH), 6.67-6.70, 6.74-6.79, 7.15-7.25 (m, 2H, 1H, 2H, aromatics).

**Tetraethyl [(4-fluorophenylamino)methyl]-1,1-bisphosphonate (2a).** 56% yield; <sup>1</sup>HNMR (CDCl<sub>3</sub>): δ 1.23-1.31 (m, 12H, CH<sub>3</sub>), 3.99-4.26 (m, 10H, CH<sub>2</sub>, CH, NH), 6.62-6.66, 6.86-6.93 (m, 2H, 2H, aromatics); MS (ESI): m/z 420 [M+Na]<sup>+</sup>; MS<sup>2</sup> m/z (%): 254 (100); m/z 396 [M-H]<sup>-</sup> MS<sup>2</sup> m/z (%): 153 (100).

**Tetraethyl [(4-chlorophenylamino)methyl]-1,1-bisphosphonate (3a).** 56% yield; <sup>1</sup>HNMR (CDCl<sub>3</sub>): δ 1.23-1.32 (m, 12H, CH<sub>3</sub>), 3.99-4.23 (m, 10H, CH<sub>2</sub>, CH, NH), 6.60-6.64, 7.10-7.15 (m, 2H, 2H, aromatics); GC-MS m/z (%): 413 [M]<sup>+</sup> (16), 415 [M+2]<sup>+</sup> (5), 276 (100).

**Tetraethyl [(4-bromophenylamino)methyl]-1,1-bisphosphonate (4a).** 83% yield; mp: 132-134 °C; <sup>1</sup>H-NMR (CDCl<sub>3</sub>): δ 1.22 -1.31 (m, 12H, CH<sub>3</sub>), 1.62-1.90 (bb 1H, NH) 4.08-4.24 (m, 9H, CH<sub>2</sub>, CH), 6.55-6.60, 7.24-7.29 (m, 2H, 2H, aromatics); GC-MS m/z (%): 459 [M+2]<sup>+</sup> (15), 457 [M]<sup>+</sup> (16), 320 [C<sub>11</sub>H<sub>16</sub>BrNO<sub>3</sub>P]<sup>+</sup> (100).

**Tetraethyl [(4-nitrophenylamino)methyl]-1,1-bisphosphonate (5a).** 89% yield; <sup>1</sup>HNMR ([D<sub>6</sub>]DMSO): δ 1.09-1.20 (m, 12H, CH<sub>3</sub>), 3.99-4.12 (m, 8H, CH<sub>2</sub>), 4.88-4.99 (m, 1H, CH), 7.05-7.08, 7.94-7.97 (m, 2H, 2H, aromatics), 7.40-7.44 (d, 1H, NH).

**Tetraethyl [(4-methylphenylamino) methyl]-1,1-bisphosphonate (6a).** 87% yield; <sup>1</sup>HNMR (CDCl<sub>3</sub>): δ 1.22-1.30 (m, 12H, CH<sub>2</sub>CH<sub>3</sub>), 2.23 (s, 3H, CH<sub>3</sub>), 3.94-3.99 (m, 1H, NH), 4.00-4.24 (m, 9H, CH<sub>2</sub>, CH), 6.59-6.61, 6.97-6.99 (m, 2H, 2H, aromatics); GC-MS m/z (%): 393 [M]<sup>+</sup> (17.5), 256 [C<sub>12</sub>H<sub>19</sub>NO<sub>3</sub>P]<sup>+</sup> (100).

**Tetraethyl [(4-trifluoromethyl-phenylamino)methyl]-1,1-bisphosphonate (7a).** 71% yield; <sup>1</sup>HNMR (CDCl<sub>3</sub>): δ 1.22-1.33 (m, 12H, CH<sub>3</sub>), 4.06-4.33 (m, 9H, CH<sub>2</sub>, CH), 4.50-4.60 (bb, 1H, NH), 6.70-6.73, 7.40-7.43 (m, 2H, 2H, aromatics); MS (ESI): m/z 470 [M+Na]<sup>+</sup>; MS<sup>2</sup> m/z (%): 304 (100); m/z 446 [M-H]<sup>-</sup> MS<sup>2</sup> m/z (%): 280 (100).

**Tetraethyl [(4-cyano-phenylamino)methyl]-1,1-bisphosphonate (8a).** 78% yield; <sup>1</sup>HNMR (CDCl<sub>3</sub>): δ 1.17-1.29 (m, 12H, CH<sub>3</sub>), 4.02-4.25 (m, 9H, CH<sub>2</sub>, CH), 4.92 (bb, 1H, NH), 6.66-6.69, 7.39-7.42 (m, 2H, 2H, aromatics). GC-MS m/z (%): 404 [M]<sup>+</sup> (10.8), 267 [C<sub>12</sub>H<sub>16</sub>N<sub>2</sub>O<sub>3</sub>P]<sup>+</sup> (100).

**Tetraethyl [(4-hydroxy-phenylamino)methyl]-1,1-bisphosphonate (9a).** 57% yield; <sup>1</sup>HNMR (CDCl<sub>3</sub>): δ 1.20-1.27 (m, 12H, CH<sub>3</sub>), 4.06-4.21 (m, 9H, CH<sub>2</sub>, CH), 5.89 (bb, 2H, OH, NH), 6.60-6.64, 6.70-6.74 (m, 2H, 2H, aromatics). GC-MS m/z (%): 395 [M]<sup>+</sup> (23.1), 258 [C<sub>11</sub>H<sub>17</sub>NO<sub>4</sub>P]<sup>+</sup> (100).

**Tetraethyl [(3-nitrophenylamino)methyl]-1,1-bisphosphonate (10a).** 53% yield; <sup>1</sup>H NMR (CDCl<sub>3</sub>): δ 1.23-1.34 (m, 12H, CH<sub>3</sub>), 4.10-4.28 (m, 9H, CH<sub>2</sub>, CH), 4.54-4.57 (m, 1H, NH), 6.97-7.01, 7.32-7.34, 7.52, 7.60-7.62 (m, 1H, 1H, 1H, 1H, aromatics); MS (ESI): m/z 447 [M+Na]<sup>+</sup>; MS<sup>2</sup> m/z (%): 419 (100); m/z 423 [M-H]<sup>-</sup> MS<sup>2</sup> m/z (%): 257 (100).

**Tetraethyl [(3-trifluoromethylphenylamino)methyl]-1,1-bisphosphonate (11a).** 82% yield; <sup>1</sup>H NMR (CDCl<sub>3</sub>): δ 1.22-1.32 (m, 12H, CH<sub>3</sub>), 4.08-4.38 (m, 9H, CH<sub>2</sub>, CH, NH), 6.83-6.89, 7.00-7.02, 7.25-7.30 (m, 2H, 1H, 1H, aromatics); MS m/z (%): 470 [M+Na]<sup>+</sup>, 304 (100); m/z 446 [M-H]<sup>-</sup> MS<sup>2</sup> m/z (%): 280 (100).

**Tetraethyl [(3-fluorophenylamino)methyl]-1,1-bisphosphonate (12a).** 55% yield; <sup>1</sup>H NMR (CDCl<sub>3</sub>): δ 1.22-1.32 (m, 12H, CH<sub>3</sub>), 4.02-4.27 (m, 10H, CH<sub>2</sub>, CH, NH), 6.37-6.48, 7.07-7.14 (m, 3H, 1H, aromatics); MS (ESI): m/z 396[M-H]<sup>-</sup>; 420 [M+Na]<sup>+</sup>; MS<sup>2</sup> m/z (%): 254 (100); m/z 396 [M-H]<sup>-</sup> MS<sup>2</sup> m/z (%): 153 (100).

**Tetraethyl [(3-bromophenylamino)methyl]-1,1-bisphosphonate (13a).** 64% yield; <sup>1</sup>H NMR (CDCl<sub>3</sub>): δ 1.24-1.33 (m, 12H, CH<sub>3</sub>), 4.02-4.20 (m, 10H, CH<sub>2</sub>, CH, NH), 6.59-6.62, 6.84-6.90, 7.00-7.06 (m, 1H, 2H, 1H, aromatics); MS (ESI): m/z 482 [M+2+Na]<sup>+</sup>, 480 [M+Na]<sup>+</sup>, MS<sup>2</sup> m/z (%): 314 (100); MS (ESI): m/z 458 [M+2-H]<sup>-</sup>, 456 [M-H]<sup>-</sup>, MS<sup>2</sup> m/z (%): 153 (100).

**Tetraethyl [(3,4-dichlorophenylamino)methyl]-1,1-bisphosphonate (14a).** 78% yield; <sup>1</sup>HNMR (CDCl<sub>3</sub>): δ 1.24-1.34 (m, 12H, CH<sub>3</sub>), 3.96-4.27 (m, 10H, CH<sub>2</sub>, CH, NH), 6.51-6.55, 6.78-6.79, 7.19-7.22 (m, 1H, 1H, 1H, aromatics); MS (GC): m/z 451 [M+4]<sup>+</sup> (1.7), 449 [M+2]<sup>+</sup> (8.6), 447 [M]<sup>+</sup> (15), 310 [C<sub>11</sub>H<sub>15</sub>Cl<sub>2</sub>NO<sub>3</sub>P]<sup>+</sup> (100).

**Tetraethyl [(4-fluoro-3-nitrophenylamino)methyl]-1,1-bisphosphonate (15a).** 64% yield; <sup>1</sup>H NMR (CDCl<sub>3</sub>): δ 1.25-1.35 (m, 12H, CH<sub>3</sub>), 3.98-4.27 (m, 9H, CH<sub>2</sub>, CH), 4.40-4.55 (bb, 1H, NH), 6.91-7.6.96, 7.08-7.14, 7.26-7.35 (m, 1H, 1H, 1H, aromatics); MS (ESI): m/z 465 [M+Na]<sup>+</sup>, MS<sup>2</sup> m/z (%): 437 (100), 441 [M-H]<sup>-</sup> MS<sup>2</sup> m/z (%): 275 (100);

**Tetraethyl [(2,4-dichlorophenylamino)methyl]-1,1-bisphosphonate (16a).** 83% yield; <sup>1</sup>HNMR (CDCl<sub>3</sub>): δ 1.24-1.33 (m, 12H, CH<sub>3</sub>), 4.05-4.12 (m, 10H, CH<sub>2</sub>, CH,

NH), 6.64-6.67, 7.15-7.18, 7.17-7.19 (m, 1H, 1H, 1H, aromatics); GC-MS *m/z* (%): 451 [M+4]<sup>+</sup> (1.3), 449 [M+2]<sup>+</sup> (7.5), 447 [M]<sup>+</sup> (11.5), 310 (100).

**Tetraethyl [(4-biphenylamino)methyl]-1,1-bisphosphonate (17a)**. 32% yield; <sup>1</sup>H NMR (CDCl<sub>3</sub>): δ 1.24-1.33 (m, 12H, CH<sub>3</sub>), 4.11-4.32 (m, 10H, CH<sub>2</sub>, CH, NH), 6.75-6.78, 7.24-7.29, 7.37-7.48, 7.51-7.55 (m, 2H, 1H, 4H, 2H, aromatics); GC-MS: *m/z* 455 [M]<sup>+</sup> (39), 318 (100).

**Tetraethyl [(4-phenoxyphenylamino)methyl]-1,1-bisphosphonate (18a)**. 66% yield; <sup>1</sup>H NMR (CDCl<sub>3</sub>): δ 1.25-1.33 (m, 12H, CH<sub>3</sub>), 4.00-4.29 (m, 10H, CH<sub>2</sub>, CH, NH), 6.67-6.72, 6.88-6.92, 6.99-7.04, 7.24-7.31 (m, 2H, 4H, 1H, 2H, aromatics); MS (ESI) 494 [M+Na]<sup>+</sup>; MS<sup>2</sup> *m/z* (%): 328 (100); *m/z* 470 [M-H]<sup>-</sup> MS<sup>2</sup> *m/z* (%): 304 (100).

**Tetraethyl [(4-(4'-chlorophenoxy)phenylamino)methyl]-1,1-bisphosphonate (19a)**. 53% yield; <sup>1</sup>H NMR (CDCl<sub>3</sub>): δ 1.25-1.33 (m, 12H, CH<sub>3</sub>), 4.04-4.25 (m, 10H, CH<sub>2</sub>, CH, NH), 6.68-6.71, 6.82-6.90, 7.20-7.26 (m, 2H, 4H, 2H, aromatics); GC-MS: *m/z* 507 [M+2]<sup>+</sup> (10), 505 [M]<sup>+</sup> (24); 368 (100).

**Tetraethyl [(4-(4'-bromophenoxy)phenylamino)methyl]-1,1-bisphosphonate (20a)**. 82% yield; <sup>1</sup>H NMR (CDCl<sub>3</sub>): δ 1.17-1.25 (m, 12H, CH<sub>3</sub>), 4.00-4.19 (m, 9H, CH<sub>2</sub>, CH), 4.41 (bb, 1H, NH), 6.64-6.72, 6.78-6.82, 7.25-7.29 (m, 4H, 2H, 2H, aromatics). GC-MS: *m/z* 550 [M+2]<sup>+</sup> (36), 548 [M]<sup>+</sup> (33), 414 (100), 412 (98).

**Tetraethyl [3-biphenylaminomethyl]-1,1-bisphosphonate (21a)**. 67% yield; <sup>1</sup>H NMR (CDCl<sub>3</sub>): δ 1.23-1.31 (m, 12H, CH<sub>3</sub>), 4.11-4.35 (m, 10H, CH<sub>2</sub>, CH, NH), 6.67-6.70, 6.90-6.91, 7.00-7.02, 7.23-7.31, 7.33-7.45, 7.53-7.57 (m, 1H, 1H, 1H, 1H, 1H, 2H, 2H, aromatics); MS (ESI): *m/z* 478 [M+Na]<sup>+</sup>; MS<sup>2</sup> *m/z* (%): 312 (100); *m/z* 454 [M-H]<sup>-</sup> MS<sup>2</sup> *m/z* (%): 288 (100).

**Tetraethyl [(naphthalen-1-ylamino)methyl]-1,1-bisphosphonate (22a)**. 81% yield; <sup>1</sup>H NMR (CDCl<sub>3</sub>): δ 1.19-1.29 (m, 12H, CH<sub>3</sub>), 4.07-4.26 (m, 8H, CH<sub>2</sub>), 4.34-4.52 (m, 1H, CH), 4.85-4.91 (m, 1H, NH) 6.76-6.79, 7.29-7.38, 7.44-7.50, 7.78-7.90 (m, 1H, 2H, 2H, 2H, aromatics); MS (ESI): *m/z* 452 [M+Na]<sup>+</sup>; MS<sup>2</sup> *m/z* (%): 286 (100); *m/z* 400 [M-Et]<sup>-</sup> MS<sup>2</sup> *m/z* (%): 153 (100).

**[(Arylamino)methyl]-1,1-bisphosphonic acids. General procedure.** Anhydrous trimethylsilylbromide (8 mmol) was carefully added to a solution of the corresponding ester in anhydrous acetonitrile (4 mL) under argon atmosphere. The resulting mixture was stirred for 24h, then CH<sub>3</sub>OH (2 mL) was added and stirring was continued for additional 30 min. The solvent was distilled off and the oil residue was washed with a mixture of hexanes and Et<sub>2</sub>O (1:1) to give the desired acids as solids in 21-96% yield.

**[(Phenylamino)methyl]-1,1-bisphosphonic acid (1) [33]**. 54 % yield; mp 114-116 °C; <sup>1</sup>H NMR ([D<sub>6</sub>]DMSO): δ 3.92 (t, *J*<sub>HP</sub> 21.46 Hz, 1H, PCHP), 6.51-6.56, 6.70-6.72, 7.01-7.07 (m, 1H, 2H, 2H, aromatics), 7.10-7.80 (bb, H, OH, NH); <sup>31</sup>P NMR ([D<sub>6</sub>]DMSO): δ=16.98 (d, *J*<sub>PH</sub> 21.37 Hz, 2P, PCHP); MS (ESI): *m/z* 266 [M-H]<sup>-</sup>; MS<sup>2</sup>: *m/z* (%): 248 (100); Anal. calcd for C<sub>7</sub>H<sub>11</sub>NO<sub>6</sub>P<sub>2</sub>·2 H<sub>2</sub>O: C 27.73%, H 4.99%, N 4.62%, found: C 27.30%, H 4.71%, N 4.47%.

**[(4-Fluorophenylamino)methyl]-1,1-bisphosphonic acid (2)**. 77% yield; mp: 168-169 °C; <sup>1</sup>H NMR ([D<sub>6</sub>]DMSO): δ 3.86 (t, *J*<sub>HP</sub> 21.46 Hz, 1H, PCHP), 6.69-6.74, 6.84-6.90 (m, 2H, 2H, aromatics), 7.60-8.60 (bb, 5H, OH, NH); <sup>31</sup>P NMR ([D<sub>6</sub>]DMSO): δ =17.03 (d, *J*<sub>PH</sub> 21.36 Hz, 2P, PCHP); MS (ESI): *m/z* 284 [M-H]<sup>-</sup>; MS<sup>2</sup>: *m/z* (%): 266 (100); Anal. calcd for C<sub>7</sub>H<sub>10</sub>FNO<sub>6</sub>P<sub>2</sub>·1/2 H<sub>2</sub>O : C 28.56%, H 3.77%, N 4.76%, found: C 28.56%, H 3.92%, N 4.44%.

**[(4-Chlorophenylamino)methyl]-1,1-bisphosphonic acid (3) [34].** 85% yield; mp: 155-156 °C; <sup>1</sup>HNMR ([D<sub>6</sub>]DMSO): δ 3.85 (t, *J*<sub>HP</sub> 21.45 Hz, 1H, PCHP), 6.72-6.74, 7.03-7.06 (m, 2H, 2H, aromatics), 6.20-7.60 (bb, OH, NH); <sup>31</sup>PNMR ([D<sub>6</sub>]DMSO): δ =16.50 (d, *J*<sub>PH</sub> 21.36 Hz, 2P, PCHP); MS (ESI): m/z 302 [M+2-H]<sup>-</sup> (32), 300 [M-H]<sup>-</sup> (100); MS<sup>2</sup>: m/z (%): 282 (100); Anal. calcd for C<sub>7</sub>H<sub>10</sub>ClNO<sub>6</sub>P<sub>2</sub>·2 H<sub>2</sub>O: C 24.90%, H 4.18%, N 4.15%, found: C 24.70%, H 4.22%, N 4.10%.

**[(4-Bromophenylamino)methyl] 1,1 bisphosphonic acid (4).** 90% yield; mp: 107-111 °C; <sup>1</sup>HNMR ([D<sub>6</sub>]DMSO): δ 3.87 (t, *J*<sub>HP</sub> 21.46 Hz 1H, PCHP), 6.67-6.70, 7.14-7.17 (m, 2H, 2H, aromatics), 8.11 (bb, 5H, NH, OH); <sup>31</sup>PNMR ([D<sub>6</sub>]DMSO): δ 16.84 (d, *J*<sub>HP</sub> 21.36 Hz, PCHP); MS (ESI): m/z (%): 344 [M-H]<sup>-</sup>; MS<sup>2</sup> (%): 328 (100); Anal. calcd for C<sub>7</sub>H<sub>10</sub>BrNO<sub>6</sub>P<sub>2</sub>: C 24.30%, H 2.91%, N 4.05%, found: C 24.42%, H 3.04%, N 4.23%.

**[(4-Nitrophenylamino)methyl]-1,1-bisphosphonic acid (5).** 37% yield; mp: 218-219 °C; <sup>1</sup>HNMR ([D<sub>6</sub>]DMSO): δ 4.10 (t, *J*<sub>HP</sub> 21.46 Hz 1H, PCHP), 6.60-8.80 (bb, 5H, OH, NH), 6.85-6.88, 7.92-7.95 (m, 2H, 2H aromatics); <sup>31</sup>P NMR ([D<sub>6</sub>]DMSO): δ =14.89 (d, *J*<sub>PH</sub> 21.36 Hz, 2P, PCHP); MS (ESI): m/z 311 [M-H]<sup>-</sup>; MS<sup>2</sup>: m/z (%): 293 (100); Anal. calcd for C<sub>7</sub>H<sub>12</sub>N<sub>2</sub>O<sub>8</sub>P<sub>2</sub>: C 26.77%, H 3.85%, N 8.92%, found: C 25.35%, H 3.86%, N 8.10%.

**[(4-Methylphenylamino)methyl]-1,1- bisphosphonic acid (6).** 96% yield; mp: 213-215 °C; <sup>1</sup>HNMR ([D<sub>6</sub>]DMSO): δ 2.12 (s, 3H, CH<sub>3</sub>), 3.84 (t, *J*<sub>HP</sub> 21.45, 1H, PCHP), 6.60-6.62, 6.84-6.87 (m, 2H, 2H, aromatics), 5.80-7.60 (bb, 5H, OH, NH); <sup>31</sup>PNMR ([D<sub>6</sub>]DMSO): δ 17.13 (d, *J*<sub>PH</sub> 21.36 Hz, 2P, PCHP); MS (ESI) m/z: 280 [M-H]<sup>-</sup>; MS<sup>2</sup> m/z (%): 262 (100); Anal. calcd for C<sub>8</sub>H<sub>13</sub>NO<sub>6</sub>P<sub>2</sub>: C 34.18%, H 4.66%, N 4.98%, found: C 34.07%, H 4.77%, N 4.75%.

**[(4-Trifluoromethylphenylamino)methyl]-1,1-bisphosphonic acid (7).** 21% yield; mp: 184-186 °C; <sup>1</sup>HNMR ([D<sub>6</sub>]DMSO): δ 4.02 (t, *J*<sub>HP</sub> 20.08 Hz, 1H, PCHP), 5.40-7.40 (bb, 5H, OH, NH), 6.76-6.96, 7.61-7.63 (m, 2H, 2H, aromatics); <sup>31</sup>PNMR ([D<sub>6</sub>]DMSO): δ =16.53 (d, *J*<sub>PH</sub> 21.36, 2P, PCHP); MS (ESI): m/z 334 [M-H]<sup>-</sup>; MS<sup>2</sup>: m/z (%): 316 (100); Anal. calcd for C<sub>8</sub>H<sub>10</sub>F<sub>3</sub>NO<sub>6</sub>P<sub>2</sub>·2 H<sub>2</sub>O: C 25.89%, H 3.80%, N 3.77%, found: C 26.01%, H 3.99%, N 3.73%.

**[(4-Cyanophenylamino)methyl]-1,1-bisphosphonic acid (8).** 93% yield; mp: 215 °C (dec); <sup>1</sup>HNMR ([D<sub>6</sub>]DMSO): δ 4.14 (t, *J*<sub>HP</sub> 20.10 Hz, 1H, PCHP), 6.85-6.88, 7.38-7.41 (m, 2H, 2H, aromatics), 9.84 (bb, 5H, OH, NH); <sup>31</sup>PNMR ([D<sub>6</sub>]DMSO): δ =15.62 (d, *J*<sub>PH</sub> 21.37, 2P, PCHP); MS (ESI): m/z 291 [M-H]<sup>-</sup>; MS<sup>2</sup>: m/z (%): 273 (100); Anal. calcd for C<sub>8</sub>H<sub>10</sub>N<sub>2</sub>O<sub>6</sub>P<sub>2</sub>·2 H<sub>2</sub>O: C 29.28%, H 4.30%, N 8.54%, found: C 29.19%, H 4.17%, N 8.96%.

**[(4-Hydroxyphenylamino)methyl]-1,1-bisphosphonic acid (9).** 92% yield; mp: 229-230 °C; <sup>1</sup>HNMR ([D<sub>6</sub>]DMSO): δ 3.71 (t, *J*<sub>HP</sub> 21.30 Hz, 1H, PCHP), 6.49-6.52, 6.57-6.60 (m, 2H, 2H, aromatics), 7.51 (bb, 6H, OH, NH). <sup>31</sup>PNMR ([D<sub>6</sub>]DMSO): δ =17.17 (d, *J*<sub>PH</sub> 21.36, 2P, PCHP); MS (ESI): m/z 282 [M-H]<sup>-</sup>; MS<sup>2</sup>: m/z (%): 264 (100); Anal. calcd for C<sub>7</sub>H<sub>11</sub>NO<sub>7</sub>P<sub>2</sub>·2 H<sub>2</sub>O: C 26.34%, H 4.74%, N 4.39%, found: C 26.53%, H 4.43%, N 4.55%.

**[(3-Nitrophenylamino)methyl]-1,1-bisphosphonic acid (10) [35].** 64% yield; mp: 204-206 °C; <sup>1</sup>HNMR ([D<sub>6</sub>]DMSO): δ 4.05 (t, *J*<sub>HP</sub> 21.46 Hz, 1H, PCHP), 7.21-7.34, 7.59 (m, 3H, 1H aromatics), 8.00-9.6 (bb, 5H, OH, NH); <sup>31</sup>PNMR ([D<sub>6</sub>]DMSO): δ =16.10 (d, *J*<sub>PH</sub> 21.36 Hz, 2P, PCHP); MS (ESI): m/z 311[M-H]<sup>-</sup>; MS<sup>2</sup>: m/z (%): 293 (100); Anal. calcd for C<sub>7</sub>H<sub>12</sub>N<sub>2</sub>O<sub>8</sub>P<sub>2</sub>·1/2 H<sub>2</sub>O : C 26.18%, H 3.45%, N 8.72%, found: C 26.05%, H 3.68%, N 8.30%.

**[(3-Trifluoromethylphenylamino)methyl]-1,1-bisphosphonic acid (11).** 70% yield; mp: 212-214 °C; <sup>1</sup>HNMR ([D<sub>6</sub>]DMSO): δ 3.96 (t, *J*<sub>HP</sub> 21.46 Hz, 1H, PCHP), 6.60-

7.80 (bb, 5H, OH, NH), 6.79-6.81, 6.97-7.06, 7.21-7.26 (m, 1H, 2H, 1H, aromatics);  $^{31}\text{P}$ NMR ( $[\text{D}_6]$ DMSO):  $\delta = 16.43$  (d,  $J_{\text{PH}} 21.37$ , 2P, PCHP); MS (ESI):  $m/z$  334  $[\text{M}-\text{H}]^-$ ;  $\text{MS}^2$ :  $m/z$  (%): 316 (100); Anal. calcd for  $\text{C}_8\text{H}_{10}\text{F}_3\text{NO}_6\text{P}_2$ : C 28.67%, H 3.01%, N 4.18%, found: C 28.90%, H 3.21%, N 3.98%.

**[(3-Fluorophenylamino)methyl]-1,1-bisphosphonic acid (12)**. 74% yield; mp: 197-198 °C;  $^1\text{H}$ NMR ( $[\text{D}_6]$ DMSO):  $\delta$  3.92 (t,  $J_{\text{HP}} 21.87$  Hz, 1H, PCHP), 6.26-6.31, 6.53-6.56, 6.99-7.07 (m, 1H, 2H, 1H, aromatics), 10.60-11.80 (bb, 5H, OH, NH);  $^{31}\text{P}$ NMR ( $[\text{D}_6]$ DMSO):  $\delta = 16.55$  (d,  $J_{\text{PH}} 21.36$ , 2P, PCHP); MS (ESI):  $m/z$  284  $[\text{M}-\text{H}]^-$ ;  $\text{MS}^2$ :  $m/z$  (%): 266 (100); Anal. calcd for  $\text{C}_7\text{H}_{10}\text{FNO}_6\text{P}_2$ : C 29.49%, H 3.54%, N 4.91%, found: C 29.88%, H 3.31%, N 4.84%.

**[(3-Bromophenylamino)methyl]-1,1-bisphosphonic acid (13) [35]**. 95% yield; mp: 185-187 °C;  $^1\text{H}$ NMR ( $[\text{D}_6]$ DMSO):  $\delta$  3.89 (t,  $J_{\text{HP}} 22.01$  Hz, 1H, PCHP), 6.65-6.74, 6.91-6.97 (m, 2H, 2H, aromatics) 10.20-11.80 (bb, 5H, OH, NH);  $^{31}\text{P}$ NMR ( $[\text{D}_6]$ DMSO):  $\delta = 16.45$  (d,  $J_{\text{PH}} 21.37$ , 2P, PCHP); MS (ESI):  $m/z$  346  $[\text{M}+2-\text{H}]^-$ , 344  $[\text{M}-\text{H}]^-$ ;  $\text{MS}^2$ :  $m/z$  (%): 326 (100); Anal. calcd for  $\text{C}_7\text{H}_{10}\text{BrNO}_6\text{P}_2$ : C 24.30%, H 2.91%, N 4.05%, found: C 24.52%, H 3.02%, N 4.43%.

**[(3,4-Dichlorophenylamino)methyl]-1,1-bisphosphonic acid (14) [34]**. 74% yield; mp: 134-135 °C;  $^1\text{H}$ NMR ( $[\text{D}_6]$ DMSO):  $\delta$  3.89 (t,  $J_{\text{HP}} 21.45$ , 1 H, PCHP), 6.72-6.75, 6.96, 7.18-7.21 (m, 1H, 1H, 1H, aromatics), 8.00-9.80 (bb, 5H, OH, NH);  $^{31}\text{P}$ NMR ( $[\text{D}_6]$ DMSO):  $\delta = 16.00$  (d,  $J_{\text{PH}} 21.37$  Hz, 2P, PCHP); MS (ESI):  $m/z$  334  $[\text{M}-\text{H}]^-$ ;  $\text{MS}^2$ :  $m/z$  (%): 316 (100); Anal. calcd for  $\text{C}_7\text{H}_9\text{Cl}_2\text{NO}_6\text{P}_2 \cdot \text{H}_2\text{O}$ : C 23.75%, H 3.13%, N 3.96%, found: C 24.16%, H 3.48%, N 4.03%.

**[(4-Fluoro-3-nitrophenylamino)methyl]-1,1-bisphosphonic acid (15)**. 85% yield; mp: 155-156 °C (dec);  $^1\text{H}$ NMR ( $[\text{D}_6]$ DMSO):  $\delta$  3.97 (t,  $J_{\text{HP}} 21.45$  Hz, 1H, PCHP), 7.21-7.24, 7.41-7.42 (m, 2H, 1H, aromatics), 8.00-10.00 (bb, 5H, OH, NH);  $^{31}\text{P}$  NMR ( $[\text{D}_6]$ DMSO):  $\delta = 16.03$  (d,  $J_{\text{PH}} 21.36$ , 2P, PCHP); MS (ESI):  $m/z$  329  $[\text{M}-\text{H}]^-$ ;  $\text{MS}^2$ :  $m/z$  (%): 311 (100); Anal. calcd for  $\text{C}_7\text{H}_{11}\text{FN}_2\text{O}_8\text{P}_2 \cdot \text{H}_2\text{O}$ : C 24.15%, H 3.18%, N 8.05%, found: C 24.51%, H 3.24%, N 8.24%.

**[(2,4-Dichlorophenylamino)methyl]-1,1-bisphosphonic acid (16) [35]**. 82 % yield; mp: 242-243 °C;  $^1\text{H}$ NMR ( $[\text{D}_6]$ DMSO):  $\delta$  3.99 (t,  $J_{\text{HP}} 20.11$  Hz, 1H, PCHP), 4.70-5.00 (bb, 1H, NH), 6.84-6.87, 7.15-7.18, 7.37-7.38 (m, 1H, 1H, 1H, aromatics), 8.60-10.00 (bb, 4H, OH);  $^{31}\text{P}$ NMR ( $[\text{D}_6]$ DMSO):  $\delta = 15.51$  (d,  $J_{\text{PH}} 18.31$ , 2P, PCHP); MS (ESI):  $m/z$  336  $[\text{M}+2-\text{H}]^-$  (65), 334  $[\text{M}-\text{H}]^-$  (100);  $\text{MS}^2$ :  $m/z$  (%): 316 (100); Anal. calcd for  $\text{C}_7\text{H}_9\text{Cl}_2\text{NO}_6\text{P}_2 \cdot 1/2 \text{H}_2\text{O}$ : C 24.37%, H 2.92%, N 4.06%, found: C 24.72%, H 2.75%, N 3.81%.

**[(4-Biphenylamino)methyl]-1,1-bisphosphonic acid (17) [35]**. 66% yield; mp: 232-233 °C;  $^1\text{H}$ NMR ( $[\text{D}_6]$ DMSO):  $\delta$  3.97 (t,  $J_{\text{HP}} 21.45$  Hz, 1H, PCHP), 6.80-6.83, 7.17-7.22, 7.33-7.40, 7.52-7.54 (m, 2H, 1H, 4H, 2H, aromatics), 6.40-8.40 (bb, 5H, OH, NH);  $^{31}\text{P}$ NMR ( $[\text{D}_6]$ DMSO):  $\delta = 16.73$  (d,  $J_{\text{PH}} 21.36$  Hz, 2P, PCHP); MS (ESI):  $m/z$  342  $[\text{M}-\text{H}]^-$ ;  $\text{MS}^2$ :  $m/z$  (%): 324 (100); Anal. calcd for  $\text{C}_{13}\text{H}_{15}\text{NO}_6\text{P}_2$ : C 45.49%, H 4.41%, N 4.08%, found: C 45.24%, H 4.48%, N 3.97%.

**[(4-Phenoxyphenylamino)methyl]-1,1-bisphosphonic acid (18)**. 80% yield; mp: 240 °C (dec);  $^1\text{H}$ NMR ( $[\text{D}_6]$ -DMSO):  $\delta = 3.88$  (t, 1H,  $J_{\text{HP}} 21.40$  Hz), 6.74-6.85, 6.96-7.01, 7.25-7.31 (m, 6H, 1H, 2H, aromatics), 7.40-8.80 (bb, 5H, OH, NH);  $^{31}\text{P}$ NMR ( $[\text{D}_6]$ -DMSO):  $\delta = 16.93$  (d, 2P,  $J_{\text{PH}} = 21.36$ ); ESI-MS,  $m/z$ : 358  $[\text{M}-\text{H}]^-$ ;  $\text{MS}^2$ ,  $m/z$  (%): 340 (100); Anal. calcd for  $\text{C}_{13}\text{H}_{15}\text{NO}_7\text{P}_2$ : C 43.47%, H 4.21%, N 3.90%, found: C 43.09%, H 4.25%, N 3.71%.

**[(4-(4'-Chlorophenoxy)phenylamino)methyl]-1,1-bisphosphonic acid (19)**. 83% yield; mp: 218-219 °C;  $^1\text{H}$ NMR ( $[\text{D}_6]$ DMSO):  $\delta$  3.90 (t,  $J_{\text{HP}} 21.45$  Hz, 1H, PCHP), 6.76-6.87, 7.30-7.35 (m, 6H, 2H, aromatics), 7.60-8.40 (bb, 5H, OH, NH);  $^{31}\text{P}$  NMR

([D<sub>6</sub>]DMSO):  $\delta$ =16.83 (d,  $J_{PH}$  21.37, 2P, PCHP); MS (ESI): m/z 392 [M-H]<sup>-</sup>; MS<sup>2</sup>: m/z (%): 374 (100); Anal. calcd for C<sub>13</sub>H<sub>14</sub>ClNO<sub>7</sub>P<sub>2</sub>: C 39.66%, H 3.58%, N 3.56%, found: C 39.94%, H 3.74%, N 3.80%.

**[(4-(4'-Bromophenoxy)phenylamino)methyl]-1,1-bisphosphonic acid (20)**. 98% yield; mp: 256-257 °C; <sup>1</sup>HNMR ([D<sub>6</sub>]DMSO):  $\delta$  3.97 (t,  $J_{HP}$  21.60 Hz, 1H, PCHP), 6.76-6.79, 7.42-7.45 (m, 6H, 2H, aromatics), 9.14 (bb, 5H, OH, NH); <sup>31</sup>P NMR ([D<sub>6</sub>]DMSO):  $\delta$ =16.90 (d,  $J_{PH}$  21.56, 2P, PCHP); MS (ESI): m/z 462 [M+2+Na]<sup>+</sup>, 460 [M+Na]<sup>+</sup>, MS<sup>2</sup>: m/z (%): 380 (100), 378 (87); Anal. calcd for C<sub>13</sub>H<sub>14</sub>BrNO<sub>7</sub>P<sub>2</sub>·H<sub>2</sub>O: C 34.23%, H 3.54%, N 3.07%, found: C 33.89%, H 3.47%, N 3.34%.

**[(3-Biphenylamino)methyl]-1,1-bisphosphonic acid (21) [36]**. 79% yield; mp: 212-214 °C; <sup>1</sup>HNMR ([D<sub>6</sub>]DMSO):  $\delta$  4.04 (t,  $J_{HP}$  21.46 Hz, 1H, PCHP), 5.80-7.00 (bb, 5H, OH, NH) 6.72-7.60 (m, 9H, aromatics); <sup>31</sup>P NMR ([D<sub>6</sub>]DMSO):  $\delta$  = 16.93 (d,  $J_{PH}$  21.37 Hz, 2P, PCHP); MS (ESI): m/z 342 [M-H]<sup>-</sup>; MS<sup>2</sup>: m/z (%): 324 (100); Anal. calcd for C<sub>13</sub>H<sub>15</sub>NO<sub>6</sub>P<sub>2</sub>·2 H<sub>2</sub>O: C 41.17%, H 5.05%, N 3.69%, found: C 41.65%, H 4.97%, N 3.77%.

**[(Naphthalen-1-ylamino)methyl]-1,1-bisphosphonic acid (22)**. 95% yield; mp 97-99 °C; <sup>1</sup>HNMR ([D<sub>6</sub>]DMSO):  $\delta$  4.16 (t,  $J_{HP}$  20.91 Hz, 1H, PCHP), 6.71-7.93 (m, 7H, aromatics), 8.40-10.00 (bb, 5H, OH, NH); <sup>31</sup>P NMR ([D<sub>6</sub>]DMSO):  $\delta$  = 16.36 (d,  $J_{PH}$  21.36 Hz, 2P, PCHP); MS (ESI): m/z 316 [M-H]<sup>-</sup>; MS<sup>2</sup>: m/z (%): 298 (100); Anal. calcd for C<sub>11</sub>H<sub>13</sub>NO<sub>6</sub>P<sub>2</sub>·2 H<sub>2</sub>O: C 37.41%, H 4.85%, N 3.97%, found: C 37.32%, H 4.44%, N 4.12%.

**[(4-Chlorophenylthio)methyl]-1,1-bisphosphonic acid (Tiludronate)**. 54% yield; mp: 174-177 °C; <sup>1</sup>HNMR ([D<sub>6</sub>]DMSO):  $\delta$  = 3.09 (t,  $J_{HP}$  19.8 Hz, 1H, PCHP), 6.20-7.80 (bb, 4H, OH), 7.30-7.33, 7.49-7.52 (m, 2H, 2H, aromatics); <sup>31</sup>P NMR ([D<sub>6</sub>]DMSO):  $\delta$  = 14.46 (d,  $J_{PH}$  18.30, 2P, PCHP); MS (ESI) m/z: 318 ([M+2]<sup>-</sup>, 34), 316 ([M]<sup>-</sup>, 100); MS<sup>2</sup> m/z (%): 299 (100); Anal. calcd for C<sub>7</sub>H<sub>9</sub>ClO<sub>6</sub>P<sub>2</sub>S: C 26.39%, H 2.85%, found: C 26.73%, H 3.05%.

**1-Hydroxy-2-(imidazol-1-yl)-ethylidene-1,1-bisphosphonic acid (Zoledronate)**. 38% yield; mp: 220-223 °C; <sup>1</sup>HNMR (D<sub>2</sub>O):  $\delta$ =4.49- 4.56 (m, 2H, NCH<sub>2</sub>C), 7.21, 7.36, 8.56 (s, 1H, 1H, 1H aromatics); <sup>31</sup>P NMR (D<sub>2</sub>O):  $\delta$ =14.83 (bb, 2P, PCP). MS (ESI) m/z: 271 [M-H]<sup>-</sup>; MS<sup>2</sup> m/z (%): 189 (100); Anal. calcd for C<sub>5</sub>H<sub>10</sub>N<sub>2</sub>O<sub>7</sub>P<sub>2</sub>·H<sub>2</sub>O: C 20.70%, H 4.17%, N 9.66%, found: C 20.41%, H 3.80%, N 9.38%.

## 4.2 Biological Methods

MMP inhibition assays.[37] Recombinant human pro-gelatinase A (pro- MMP-2) and enzymes consisting of the catalytic domain of MMP-9 and MMP-14 were purchased from Calbiochem, while catalytic domain of MMP-8 was purchased from Biomol. Pro-MMP-2 was activated immediately prior to use with *p*-aminophenylmercuric acetate (APMA, 2 mM) for 1 h at 37 °C. The assays were performed in triplicate in a total volume of 100  $\mu$ L per well in 96-well microtitre plates (Corning, white, NBS). For assay measurements, inhibitor stock solutions (DMSO, 10 mM) were diluted to six different concentrations (0.1 nM-100  $\mu$ M) in fluorometric assay buffer (50 mM Tris-HCl, pH 7.5, 200 mM NaCl, 1 mM CaCl<sub>2</sub>, 1  $\mu$ M ZnCl<sub>2</sub>, 0.05% NaN<sub>3</sub>, 0.05% Brij-35, and 1% DMSO). Activated enzyme and inhibitor solutions were incubated in the assay buffer for 30 min at 25 °C before the addition of the fluorogenic substrate solution (Mca-Pro-Leu-Gly-Leu-Dpa-Ala-Arg-NH<sub>2</sub>, Calbiochem, 2.5  $\mu$ M final concentration). After further incubation for 2-4 h at 37 °C, the hydrolysis was stopped by the addition of a 3% acetic acid solution, and the fluorescence was

measured ( $\lambda_{\text{ex}}=340$  nm,  $\lambda_{\text{em}}=405$  nm) using a PERKIN–ELMER Victor V3 plate reader. Control wells lacked inhibitor. The MMP inhibition activity was expressed in relative fluorescent units (RFU). Percent of inhibition was calculated from control reactions without the inhibitor, and  $\text{IC}_{50}$  values were determined using GraphPad PRISM version 5.0 software.[38]

MTT assay for cell viability.[39, 40] The murine macrophage-like J774 A.1 and human liver carcinoma HepG2 cell lines were obtained from the ITCC (Genova, Italy). Cells were grown in DMEM (J774 A.1) or MEM (HepG2) medium supplemented with 10% fetal bovine serum, 10  $\text{U mL}^{-1}$  penicillin, 100  $\text{mg mL}^{-1}$  streptomycin, and 2 mM L-glutamine in a 5%  $\text{CO}_2$  atmosphere at 37 °C. Cells were seeded at a density of  $1\text{--}5 \cdot 10^4$  cells/well into 96-well flat bottom culture plates containing 50  $\mu\text{L}$  of the test compounds, previously half-log serially diluted (from 0.316  $\mu\text{M}$  to 100 nM), in a final volume of 100  $\mu\text{L}$ . The bisphosphonates were dissolved in DMSO (1% final concentration; DMSO carrier had no effect on cell proliferation). Control wells lacked inhibitor. After 48 h of incubation at 37°C in a 5%  $\text{CO}_2$  atmosphere, 3-(4,5-dimethylthiazole-2-yl)-2,5-diphenyltetrazolium bromide (MTT, 5  $\text{mg mL}^{-1}$  stock solution) was added to a final concentration of 0.5  $\text{mg mL}^{-1}$ . As control for background absorbance, six wells of cells were lysed by adding Triton X-100 (0.1% v/v final concentration) immediately prior to the addition of MTT reagent. After incubation under the same conditions for further 3–4 h, the culture medium was removed, the insoluble product dissolved by the addition of 100  $\mu\text{L}$  of solvent (50% DMSO, 50% EtOH v/v), and the absorbance of the well was measured at 570 nm using a PERKIN–ELMER Victor V<sup>3</sup> plate reader. Cell growth inhibition was then calculated using Equation (1),

$$V\% = \frac{A - A_b}{A_c - A_b} \times 100 \quad (1)$$

where V% is the percentage of cell viability, A is the absorbance of treated cultures,  $A_b$  is the absorbance of background control, and  $A_c$  is the absorbance of control cultures.  $\text{IC}_{50}$  values were determined from dose-response curves using GraphPad PRISM version 5.0.

#### 4.3 Hydroxyapatite affinity measurement

A solution of each synthesized bisphosphonic acid (100  $\mu\text{M}$ ) in Tris-HCl buffer (50 mM pH=7.5) was prepared. It was divided into two aliquots (5 ml) in order to obtain the experiment in duplicate, added and stirred with HAP (4 mg) at 37 °C.

After 2 h, the mixture aliquots were centrifuged (10 min, 8000 rpm), the decanted solutions were filtered (0.22  $\mu\text{m}$  syringe's filter) and the absorbance of the clear solutions was recorded and quantified by calibration lines. The resulting  $\lambda_{\text{max}}$ ,  $\epsilon$  value, angular coefficient of the calibration line (m) and the coefficient of determination ( $R^2$ ) related are listed in the Supporting Information.

#### 4.4 Computational methods

All calculations were performed on a DELL T5500 workstation, equipped with two Intel® Xeon® E5630 2.53 GHz processors.

All compounds were manually built in Maestro version 9.3.5 [41], exploiting the Built facility. Ligands were submitted to Epik v. 2.3 [41-43] to calculate the protonation

state at neutral pH. All structures were minimized to a derivative convergence of  $0.001 \text{ kJ}\text{\AA}^{-1}\text{mol}^{-1}$ , using the Truncated Newton Conjugate Gradient (TNCG) minimization algorithm, the OPLS2005 force field, and the GB/SA water solvation model implemented in MacroModel version 9.9.[41]

Conformational searches, applying the Mixed torsional/Low-mode sampling and the automatic set-up protocol, were carried out on all minimized ligand structures in order to obtain the global minimum geometry of each molecule, which was then used as the starting conformation for docking calculations with Glide version 5.8.[41, 44-46]

Three-dimensional coordinates of MMP-2 (PDB ID: 1QIB), MMP-8 (PDB ID: 1ZVX), MMP-9 (PDB ID: 1GKC) and MMP-14 (PDB ID: 3MA2), were downloaded from the Brookhaven Protein Data Bank.[38]

MMPs 3D structures were submitted to the Protein Preparation routine in Maestro that allows fixing of receptor structures, eliminating water molecules and possible ligands, fixing bond orders, adding hydrogen atoms, and ionizing lysine, arginine, glutamate, and aspartate residues. To optimize the hydrogen bond network, histidine tautomers and ionization states were predicted,  $180^\circ$  rotations of the terminal  $\chi$  angle of Asn, Gln, and His residues were assigned, and hydroxyl and thiol hydrogen atoms were sampled. For each structure, a brief relaxation was performed using an all-atom constrained minimization carried out with the OPLS-2005 force field to reduce steric clashes that may exist in the original PDB structures. The minimization was terminated when the energy converged or the root mean square deviation (RMSD) reached a maximum cut-off of  $0.30 \text{ \AA}$ .

Glide energy grids were generated for each receptor structure using the MMP-8 crystallographic ligand as the center of the grid as a reference for all MMPs. The size of the box was determined automatically on the basis of the ligand dimensions. The global minimum geometry of each ligand was submitted to flexible docking calculations in the previously prepared proteins. The van der Waals radii for non-polar ligand atoms were scaled by a factor of 0.8, thereby decreasing penalties for close contacts. Receptor atoms were not scaled. A first docking run was carried out applying the Standard Precision (SP) settings of Glide. Ten poses were saved and the best ranking pose for each ligand was submitted to minimization process applying the Embrace module of MacroModel. Embrace performs a multiple minimization on each pre-positioned ligand and the receptor. All structures were fully minimized to a gradient convergence of  $0.05 \text{ kJ}\text{\AA}^{-1}\text{mol}^{-1}$ , using the PRCG minimization algorithm, the OPLS2005 force field and the GB/SA water solvation model. The Energy difference mode was applied to calculate the binding energy. Physicochemical properties were calculated using Canvas [41].

### **Acknowledgements**

The authors are grateful to Dr. Maria Teresa Rubino for preliminary experiments. This work was accomplished thanks to the financial support of the Ministero dell'Istruzione, dell'Università e della Ricerca (MIUR 2007 JERJPC\_003).

### **Keywords**

Matrix metalloproteinases inhibitors, zinc binding group, bone targeting, bisphosphonates

### **References**

- [1] E.T. Keller, J. Brown, Prostate cancer bone metastases promote both osteolytic and osteoblastic activity, *J. Cell. Biochem.* 91 (2004) 718-729.
- [2] C.J. Logothetis, S.H. Lin, Osteoblasts in prostate cancer metastasis to bone, *Nat. Rev. Cancer* 5 (2005) 21-28.
- [3] P. Clezardin, A. Teti, Bone metastasis: pathogenesis and therapeutic implications, *Clin. Exp. Metastasis* 24 (2007) 599-608.
- [4] C.C. Lynch, Matrix metalloproteinases as master regulators of the vicious cycle of bone metastasis, *Bone* 48 (2011) 44-53.
- [5] J.A. Nemeth, R. Yousif, M. Herzog, M. Che, J. Upadhyay, B. Shekarriz, S. Bhagat, C. Mullins, R. Fridman, M.L. Cher, Matrix metalloproteinase activity, bone matrix turnover, and tumor cell proliferation in prostate cancer bone metastasis, *J. Natl. Cancer Inst.* 94 (2002) 17-25.
- [6] S. Varghese, Matrix metalloproteinases and their inhibitors in bone: an overview of regulation and functions, *Front. Biosci.* 11 (2006) 2949-2966.
- [7] S. Zhang, G. Gangal, H. Uludag, 'Magic bullets' for bone diseases: progress in rational design of bone-seeking medicinal agents, *Chem. Soc. Rev.* 36 (2007) 507-531.
- [8] R.K. Yadav, S.P. Gupta, P.K. Sharma, V.M. Patil, Recent advances in studies on hydroxamates as matrix metalloproteinase inhibitors: A review, *Curr. Med. Chem.* 18 (2011) 1704-1722.
- [9] F.E. Jacobsen, J.A. Lewis, S.M. Cohen, The design of inhibitors for medicinally relevant metalloproteins, *ChemMedChem* 2 (2007) 152-171.
- [10] J.W. Skiles, N.C. Gonnella, A.Y. Jeng, The design, structure, and therapeutic application of matrix metalloproteinase inhibitors, *Curr. Med. Chem.* 8 (2001) 425-474.
- [11] B.G. Rao, Recent developments in the design of specific Matrix Metalloproteinase inhibitors aided by structural and computational studies, *Curr. Pharm. Des.* 11 (2005) 295-322.
- [12] O. Nicolotti, M. Catto, I. Giangreco, M. Barletta, F. Leonetti, A. Stefanachi, L. Pisani, S. Cellamare, P. Tortorella, F. Loiodice, A. Carotti, Design, synthesis and biological evaluation of 5-hydroxy, 5-substituted-pyrimidine-2,4,6-triones as potent inhibitors of gelatinases MMP-2 and MMP-9, *Eur. J. Med. Chem.* 58 (2012) 368-376.
- [13] M. Agamennone, C. Campestre, S. Preziuso, V. Consalvi, M. Crucianelli, F. Mazza, V. Politi, R. Ragno, P. Tortorella, C. Gallina, Synthesis and evaluation of new tripeptide phosphonate inhibitors of MMP-8 and MMP-2, *Eur. J. Med. Chem.* 40 (2005) 271-279.
- [14] M.T. Rubino, D. Maggi, A. Laghezza, F. Loiodice, P. Tortorella, Identification of novel matrix metalloproteinase inhibitors by screening of phenol fragments library, *Arch. Pharm.* 344 (2011) 557-563.
- [15] M.T. Rubino, M. Agamennone, C. Campestre, G. Fracchiolla, A. Laghezza, F. Loiodice, E. Nuti, A. Rossello, P. Tortorella, Synthesis, SAR, and biological evaluation of alpha-sulfonylphosphonic acids as selective matrix metalloproteinase inhibitors, *ChemMedChem* 4 (2009) 352-362.
- [16] A.R. Folgueras, A. Fueyo, O. Garcia-Suarez, J. Cox, A. Astudillo, P. Tortorella, C. Campestre, A. Gutierrez-Fernandez, M. Fanjul-Fernandez, C.J. Pennington, D.R. Edwards, C.M. Overall, C. Lopez-Otin, Collagenase-2 deficiency or inhibition impairs experimental autoimmune encephalomyelitis in mice, *J. Biol. Chem.*, 283 (2008) 9465-9474.
- [17] A. Biasone, P. Tortorella, C. Campestre, M. Agamennone, S. Preziuso, M. Chiappini, E. Nuti, P. Carelli, A. Rossello, F. Mazza, C. Gallina, alpha-

- Biphenylsulfonamino 2-methylpropyl phosphonates: Enantioselective synthesis and selective inhibition of MMPs, *Bioorg. Med. Chem. Lett.* 15 (2007) 791-799.
- [18] G. Pochetti, E. Gavuzzo, C. Campestre, M. Agamennone, P. Tortorella, V. Consalvi, C. Gallina, O. Hiller, H. Tschesche, P.A. Tucker, F. Mazza, Structural insight into the stereoselective inhibition of MMP-8 by enantiomeric sulfonamide phosphonates, *J. Med. Chem.* 49 (2006) 923-931.
- [19] C. Campestre, M. Agamennone, P. Tortorella, S. Preziuso, A. Biasone, E. Gavuzzo, G. Pochetti, F. Mazza, O. Hiller, H. Tschesche, V. Consalvi, C. Gallina, N-hydroxyurea as zinc binding group in matrix metalloproteinase inhibition: Mode of binding in a complex with MMP-8, *Bioorg. Med. Chem. Lett.* 16 (2006) 20-24.
- [20] M.T. Rubino, M. Agamennone, C. Campestre, P. Campiglia, V. Cremasco, R. Faccio, A. Laghezza, F. Loiodice, D. Maggi, E. Panza, A. Rossello, P. Tortorella, Biphenyl sulfonamino methyl bisphosphonic acids as inhibitors of matrix metalloproteinases and bone resorption, *ChemMedChem* 6 (2011) 1258-1268.
- [21] S. Lenevich, M.D. Distefano, Nuclear magnetic resonance-based quantification of organic diphosphates, *Anal. Biochem.* 408 (2011) 316-320.
- [22] R.G.G. Russell, M.A. Lawson, Z. Xia, B.L. Barnett, J.T. Triffitt, R.J. Phipps, J.E. Dunford, R.M. Locklin, F.H. Ebetino, Differences between bisphosphonates in binding affinities for hydroxyapatite, *J. Biomed. Mater. Res., Part B* 92B (2010) 149-155.
- [23] W. Jahnke, C. Henry, An in vitro assay to measure targeted drug delivery to bone mineral, *ChemMedChem* 5 (2010) 770-776.
- [24] A. Balakrishna, M.V. Narayana Reddy, P.V. Rao, M.A. Kumar, B.S. Kumar, S.K. Nayak, C.S. Reddy, Synthesis and bio-activity evaluation of tetraphenyl(phenylamino) methylene bisphosphonates as antioxidant agents and as potent inhibitors of osteoclasts in vitro, *Eur. J. Med. Chem.* 46 (2011) 1798-1802.
- [25] J.G. Topliss, Quantitative structure-activity relationships of drugs, *J. Med. Chem. Academic Press NY Chap.1* (1983).
- [26] J. Cai, Y. Duan, J. Yu, J. Chen, M. Chao, M. Ji, Bone-targeting glycol and NSAIDS ester prodrugs of rhein: synthesis, hydroxyapatite affinity, stability, anti-inflammatory, ulcerogenicity index and pharmacokinetics studies, *Eur. J. Med. Chem.* 55 (2012) 409-419.
- [27] J. Frant, A. Veerendhar, T. Chernilovsky, S. Nedvetzki, O. Vaksman, A. Hoffman, E. Breuer, R. Reich, Orally active, antimetastatic, nontoxic diphenyl ether-derived carbamoylphosphonate matrix metalloproteinase inhibitors, *ChemMedChem* 6 (2011) 1471-1477.
- [28] C. T. Leu, E. Luegmayr, L. P. Freedman, G. A. Rodan, A. A. Reszka Relative binding affinities of bisphosphonates for human bone and relationship to antiresorptive efficacy, *Bone* 38 (2006) 628-636.
- [29] D. F. Veber, S. R. Johnson, H. Y. Cheng, B. R. Smith, K. W. Ward, K. D. Kopple Molecular properties that influence the oral bioavailability of drug candidates, *J. Med. Chem.* 45 (2002) 2615-2623.
- [30] H. Murakami, N. Takahashi, T. Sasaki, N. Udagawa, S. Tanaka, I. Nakamura, D. Zhang, A. Barbier, T. Suda, A possible mechanism of the specific action of bisphosphonates on osteoclasts: Tiludronate preferentially affects polarized osteoclasts having ruffled borders, *Bone* 17 (1995) 137-144.
- [31] I.R. Greig, A.I. Idris, S.H. Ralston, R.J. van't Hof, Development and characterization of biphenylsulfonamides as novel inhibitors of bone resorption, *J. Med. Chem.* 49 (2006) 7487-7492.

- [32] S.P. Luckman, F.P. Coxon, F.H. Ebetino, R.G. Russell, M.J. Rogers, Heterocycle-containing bisphosphonates cause apoptosis and inhibit bone resorption by preventing protein prenylation: evidence from structure-activity relationships in J774 macrophages, *J. Bone Miner. Res.* 13 (1998) 1668-1678.
- [33] M.S. Wu, R.Y. Chen, Y. Huang Convenient synthesis of analogs of aminomethylene gem-diphosphonic acid from amines without catalyst, *Synthetic Commun.* 34 (2004) 1393-1398.
- [34] G. Forlani, A. Occhipinti, L. Berlicki, G. Dziedziola, A. Wieczorek, P. Kafarski Tailoring the structure of aminobisphosphonates to target plant P5C reductase, *J. Agric. Food Chem.* 56 (2008) 3193-3199.
- [35] E. Kotsikorou, Y. Song, J. M. Chan, S. Faelens, Z. Tovian, E. Broderick, N. Bakalara, R. Docampo, E. Oldfield Bisphosphonate inhibition of the exopolyphosphatase activity of the *Trypanosoma brucei* soluble vacuolar pyrophosphatase, *J. Med. Chem.* 48 (2005) 6128-6139.
- [36] Y. S. Lin, J. Park, J. W. De Schutter, X. F. Huang, A. M. Berghuis, M. Sebag, Y. S. Tsantrizos Design and synthesis of active site inhibitors of the human farnesyl pyrophosphate synthase: apoptosis and inhibition of ERK phosphorylation in multiple myeloma cells, *J. Med. Chem.* 55 (2012) 3201-3215.
- [37] G. Murphy, T. Crabbe, Gelatinases A and B, *Methods Enzymol.* 248 (1995) 470-484.
- [38] H.M. Berman, J. Westbrook, Z. Feng, G. Gilliland, T.N. Bhat, H. Weissig, I.N. Shindyalov, P.E. Bourne, The Protein Data Bank. *Nucleic Acids Res.*, 28 (2000) 235-242.
- [39] S.P. Luckman, F.H. Ebetino, R.G. Russell, M.J. Rogers, Heterocycle-containing bisphosphonates cause apoptosis and inhibit bone resorption by preventing protein prenylation: evidence from structure-activity relationships in J774 macrophages, *J. Bone Miner. Res.* 13 (1998) 1668-1678.
- [40] ATCC, posting date. ATCC, Manassas, VA (USA); <http://www.atcc.org>.
- [41] Maestro v. 9.3.5; Epik, version 2.3; MacroModel, version 9.9; Glide, version 5.8; Canvas v. 1.3, Schrödinger, LLC, New York, NY, 2012. (2012).
- [42] J.R. Greenwood, D. Calkins, A.P. Sullivan, J.C. Shelley, Towards the comprehensive, rapid, and accurate prediction of the favorable tautomeric states of drug-like molecules in aqueous solution, *J. Comput. Aided Mol. Des.* 24 (2010) 591-604.
- [43] J.C. Shelley, A. Cholleti, L. Frye, J.R. Greenwood, M.R. Timlin, M. Uchimaya, Epik: a software program for pKa prediction and protonation state generation for drug-like molecules, *J. Comp. Aided Mol. Design* 21 (2007) 681-691.
- [44] R.A. Friesner, R.B. Murphy, M.P. Repasky, L.L. Frye, J.R. Greenwood, T.A. Halgren, P.C. Sanschagrin, D.T. Mainz, Extra precision glide: docking and scoring incorporating a model of hydrophobic enclosure for protein-ligand complexes, *J. Med. Chem.* 49 (2006) 6177-6196.
- [45] T.A. Halgren, R.B. Murphy, R.A. Friesner, H.S. Beard, L.L. Frye, W.T. Pollard, J.L. Banks, Glide: a new approach for rapid, accurate docking and scoring. 2. Enrichment factors in database screening, *J. Med. Chem.* 47 (2004) 1750-1759.
- [46] R.A. Friesner, J.L. Banks, R.B. Murphy, T.A. Halgren, J.J. Klicic, D.T. Mainz, M.P. Repasky, E.H. Knoll, D.E. Shaw, M. Shelley, J.K. Perry, P. Francis, P.S. Shenkin, Glide: a new approach for rapid, accurate docking and scoring. 1. Method and assessment of docking accuracy, *J. Med. Chem.* 47 (2004) 1739-1749.

### Captions

**Figure 1.** Chemical structures of bisphosphonate derivatives. Substituents X in **1–21** are presented in Table 1

**Scheme 1.** a) 160°C, 3-4h; b) (CH<sub>3</sub>)<sub>3</sub>SiBr, CH<sub>3</sub>CN, 48-72h, MeOH.

**Figure 2. Black and White** Superimposition of docked poses of compounds **4** (light grey C atoms) and **5** (dark grey C atoms) into MMP-2. MMP-2 structure is represented as grey cartoon. Zinc ion is depicted as a sphere. Ligands and most relevant receptor residues are represented as sticks. H-bonds are represented as dashed lines.

**Figure 2.** Superimposition of docked poses of compounds **4** (orange C atoms) and **5** (blue C atoms) into MMP-2. MMP-2 structure is represented as grey cartoon. Zinc ion is depicted as a purple sphere. Ligands and most relevant receptor residues are represented as sticks. H-bonds are represented as green dashed lines.

**Figure 3. Black and White** Docked pose of compound **22** into MMP-9. MMP-9 structure is represented as dark grey cartoon. Zinc ion is depicted as a sphere. Ligands and most relevant receptor residues are represented as sticks. H-bonds are represented as dashed lines.

**Figure 3.** Docked pose of compound **22** into MMP-9. MMP-9 structure is represented as dark grey cartoon. Zinc ion is depicted as a purple sphere. Ligands and most relevant receptor residues are represented as sticks. H-bonds are represented as green dashed lines.

**Figure 4. Black and White** Superimposition of docked poses of compounds **10** (light grey C atoms) and **11** (dark grey C atoms) into MMP-2. MMP-2 structure is represented as grey cartoon. Zinc ion is depicted as a sphere and ligands as sticks. H-bonds are represented as dashed lines. For clarity the molecular surface of S1 and S3 sites is shown.

**Figure 4.** Superimposition of docked poses of compounds **10** (magenta C atoms) and **11** (yellow C atoms) into MMP-2. MMP-2 structure is represented as grey cartoon. Zinc ion is depicted as a purple sphere and ligands as sticks. H-bonds are represented as green dashed lines. For clarity the molecular surface of S1 and S3 sites is shown.

**Figure 5.** Graphical representation of cell % viability derived from MTT assay of compounds **1-22** in comparison with tiludronate at 100 µM. The side-by-side comparison between BP-MMPIs effects on J774 mouse macrophage cell line and HepG2 hepatocellular carcinoma underlines the selectivity of action of BPs. Data processed by one-way analysis of variance (Bonferroni's Multiple Comparison Test) show that each BP-MMPI presents a statistical significance of P<0.001 from control.

**Table 1.** MMP inhibition activity ( $IC_{50}$   $\mu$ M)

Entry	X	MMP-2	MMP-8	MMP-9	MMP-14
<i>tiludronate</i>		7.2 $\pm$ 0.5	32 $\pm$ 3	>100	30.5 $\pm$ 1.6
<i>zoledronate</i>		7.0 $\pm$ 1.3	17.6 $\pm$ 4.6	52 $\pm$ 6	12.6 $\pm$ 0.1
<b>1</b>	H	>100	>100	>100	>100
<b>2</b>	4-F	28.2 $\pm$ 1.3	>100	>100	>100
<b>3</b>	4-Cl	>100	>100	>100	>100
<b>4</b>	4-Br	6 $\pm$ 3	2.4 $\pm$ 0.4	30 $\pm$ 7	3.9 $\pm$ 1.7
<b>5</b>	4-NO <sub>2</sub>	20 $\pm$ 10	15 $\pm$ 2	20 $\pm$ 6	26 $\pm$ 5
<b>6</b>	4-CH <sub>3</sub>	>100	36 $\pm$ 4	>100	>100
<b>7</b>	4-CF <sub>3</sub>	15 $\pm$ 4	>100	>100	>100
<b>8</b>	4-CN	36 $\pm$ 4	>100	>100	>100
<b>9</b>	4-OH	6.6 $\pm$ 0.7	>100	>100	>100
<b>10</b>	3-NO <sub>2</sub>	15.5 $\pm$ 0.5	>100	>100	>100
<b>11</b>	3-CF <sub>3</sub>	20.8 $\pm$ 1.2	>100	>100	>100
<b>12</b>	3-F	42 $\pm$ 8	>100	>100	>100
<b>13</b>	3-Br	37.4 $\pm$ 2.1	>100	>100	>100
<b>14</b>	3,4-Cl	>100	25.5 $\pm$ 0.4	>100	20 $\pm$ 5
<b>15</b>	3-NO <sub>2</sub> , 4-F	25 $\pm$ 3	>100	>100	>100
<b>16</b>	2,4-Cl	>100	>100	>100	>100
<b>17</b>	4-Ph	>100	30 $\pm$ 5	>100	33.5 $\pm$ 2.1
<b>18</b>	4-Ph-O	2.8 $\pm$ 0.4	44 $\pm$ 4	>100	43 $\pm$ 14
<b>19</b>	4-(4-Cl-PhO)	2.1 $\pm$ 0.5	39.9 $\pm$ 0.2	55 $\pm$ 18	76 $\pm$ 7
<b>20</b>	4-(4-Br-PhO)	2.8 $\pm$ 0.1	43 $\pm$ 3	87 $\pm$ 4	49.5 $\pm$ 2.3
<b>21</b>	3-Ph	>100	52 $\pm$ 10	>100	40 $\pm$ 4
<b>22</b>		6.4 $\pm$ 1.4	61 $\pm$ 20	6.0 $\pm$ 1.2	69 $\pm$ 8

**Table 2.** In vitro HAP binding affinity

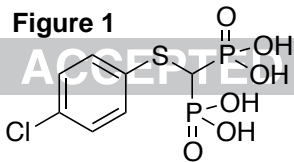
<b>Entry</b>	<b>% adsorbed</b>
tiludronate	51.5±2.1
<b>1</b>	58±5
<b>2</b>	61.2±0.1
<b>3</b>	64.2±0.6
<b>4</b>	49±4
<b>5</b>	76.0±1.8
<b>6</b>	23.9±0.3
<b>7</b>	42.5±0.1
<b>8</b>	76.0±0.6
<b>9</b>	88.4±0.1
<b>10</b>	57.8±1.6
<b>11</b>	50.3±1.6
<b>12</b>	63.6±0.7
<b>13</b>	70.1±1.1
<b>14</b>	53.5±0.5
<b>15</b>	66.2±2.8
<b>16</b>	56.8±1.3
<b>17</b>	60±7
<b>18</b>	66.2±0.2
<b>19</b>	52.1±0.6
<b>20</b>	60.7±1.6
<b>21</b>	66.4±0.3
<b>22</b>	51.6±0.1

Table 3. Physicochemical properties calculated for tested compounds.

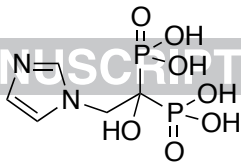
Name	mol MW	HBA <sup>a</sup>	HBD <sup>b</sup>	AlogP	RB <sup>c</sup>	PSA <sup>d</sup>	QPlogSw <sup>e</sup>
Tiludronate	318.6	2	2	0.82	4	165.6	-1.02
Zoledronate	257.1	3	3	-2.61	4	170.2	1.21
1	267.1	2	3	-0.57	4	152.4	-0.82
2	285.1	2	3	-0.37	4	152.4	-1.16
3	301.6	2	3	0.09	4	152.4	-1.51
4	346.0	2	3	0.18	4	152.4	-1.61
5	312.1	2	3	-0.68	5	195.5	-0.89
6	281.1	2	3	-0.09	4	152.4	-1.27
7	335.1	2	3	0.37	5	152.4	-2.10
8	292.1	3	3	-0.69	4	176.2	-1.78
9	282.1	3	4	-0.84	4	172.6	-0.93
10	312.1	2	3	-0.68	5	195.5	-0.88
11	335.1	2	3	0.37	5	152.4	-2.18
12	285.1	2	3	-0.37	4	152.4	-1.16
13	346.0	2	3	0.18	4	152.4	-1.61
14	336.0	2	3	0.76	4	152.4	-2.08
15	330.1	2	3	-0.47	5	195.5	-1.11
16	336.0	2	3	0.76	4	152.4	-1.78
17	343.2	2	3	0.95	5	152.4	-2.54
18	359.2	3	3	0.99	6	161.6	-2.46
19	393.7	3	3	1.65	6	161.6	-3.18
20	438.1	3	3	1.74	6	161.6	-3.25
21	343.2	2	3	0.95	5	152.4	-2.51
22	317.2	2	3	0.34	4	152.4	-1.61

**Figure 1**

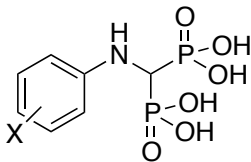
ACCEPTED MANUSCRIPT



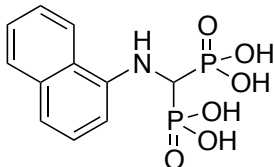
tiludronate



zoledronate

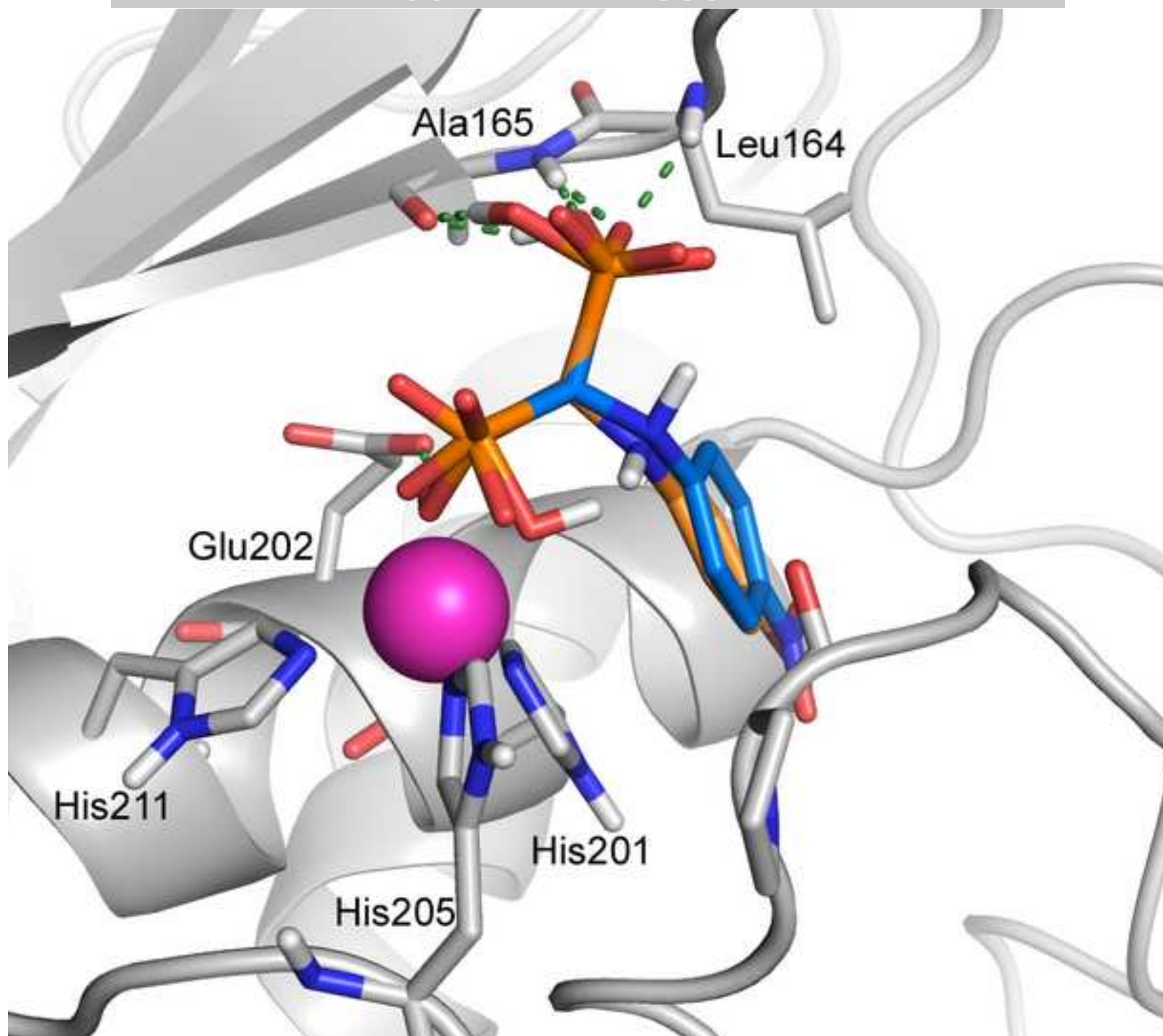


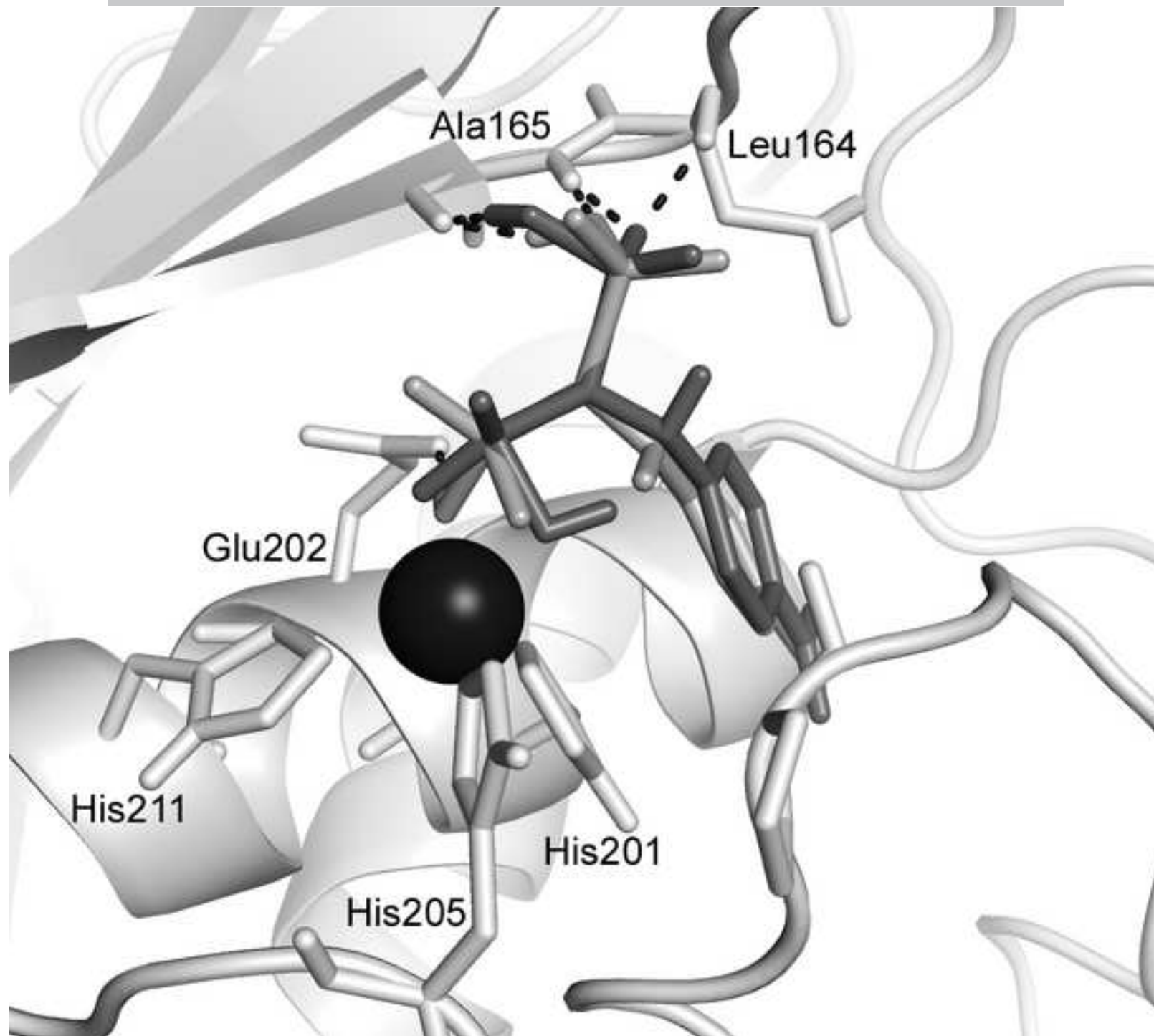
1-21

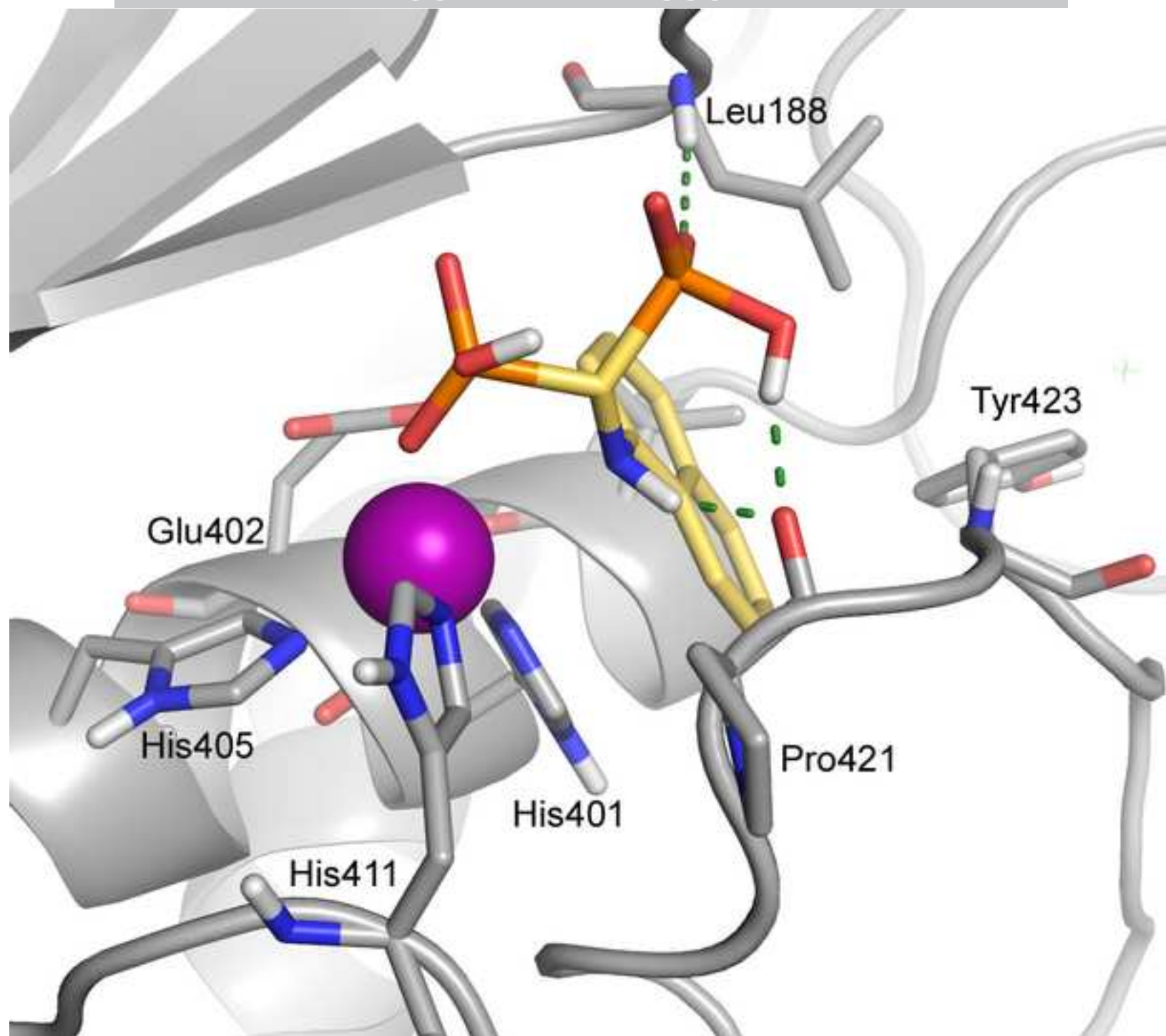


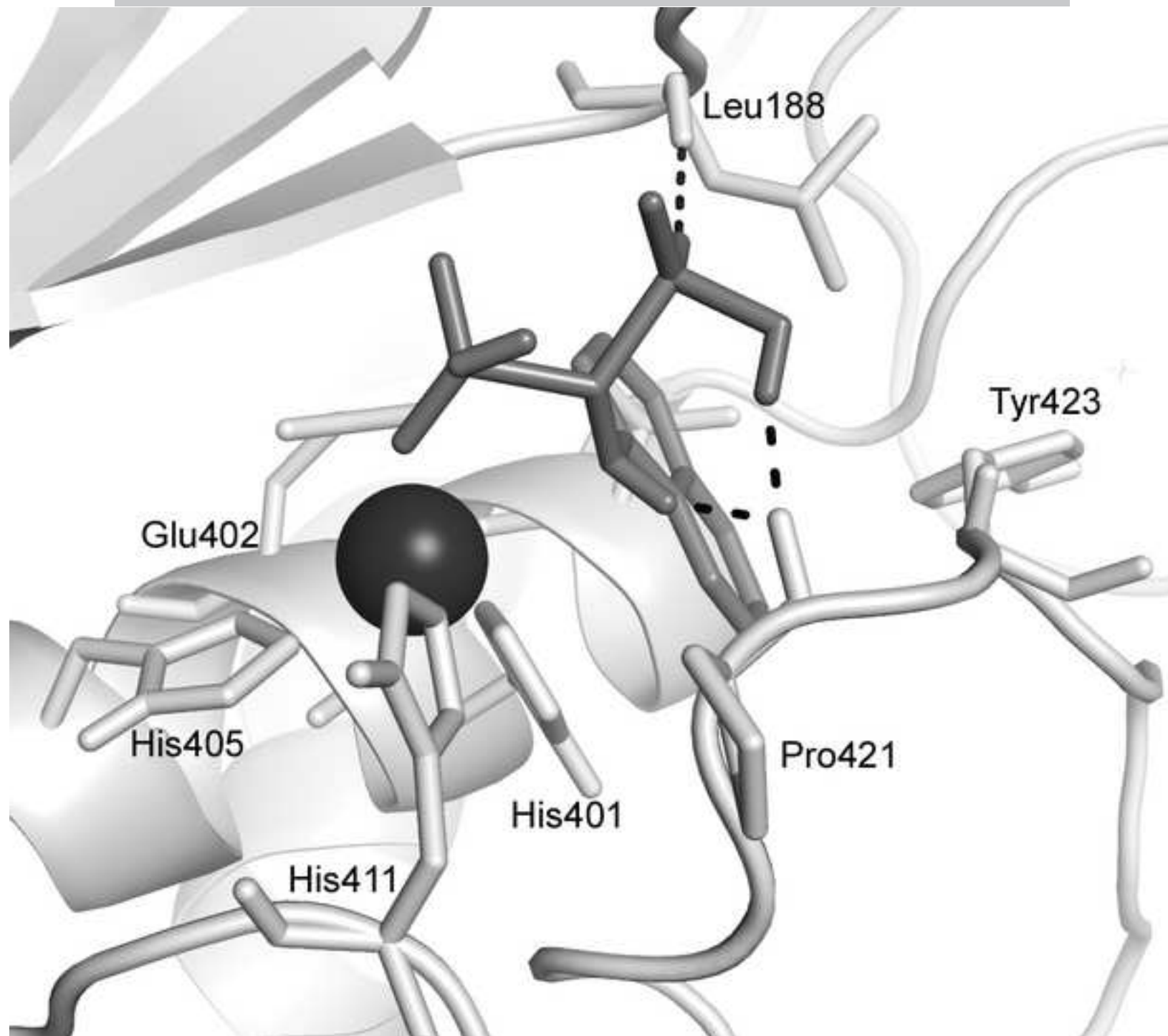
22

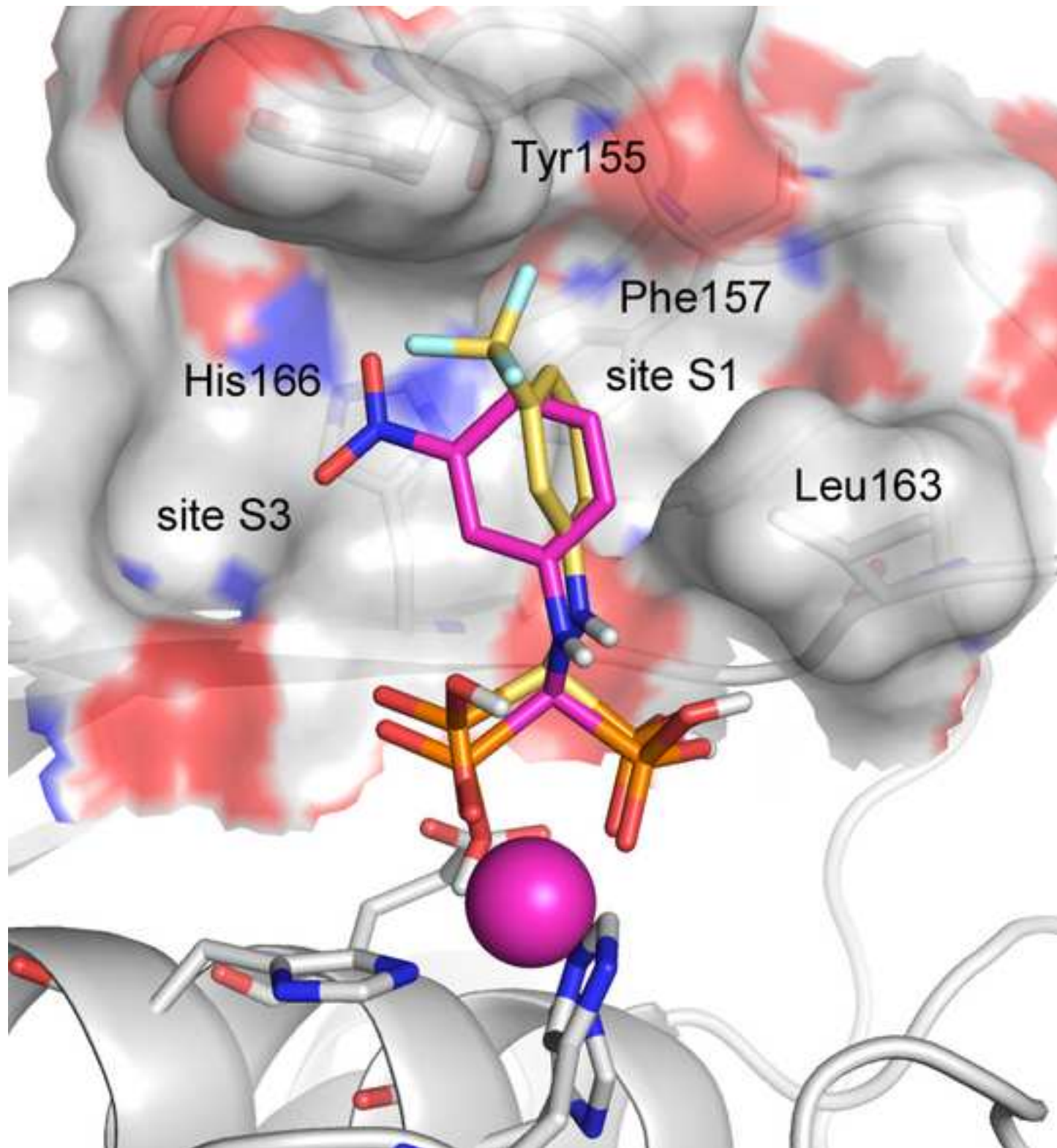












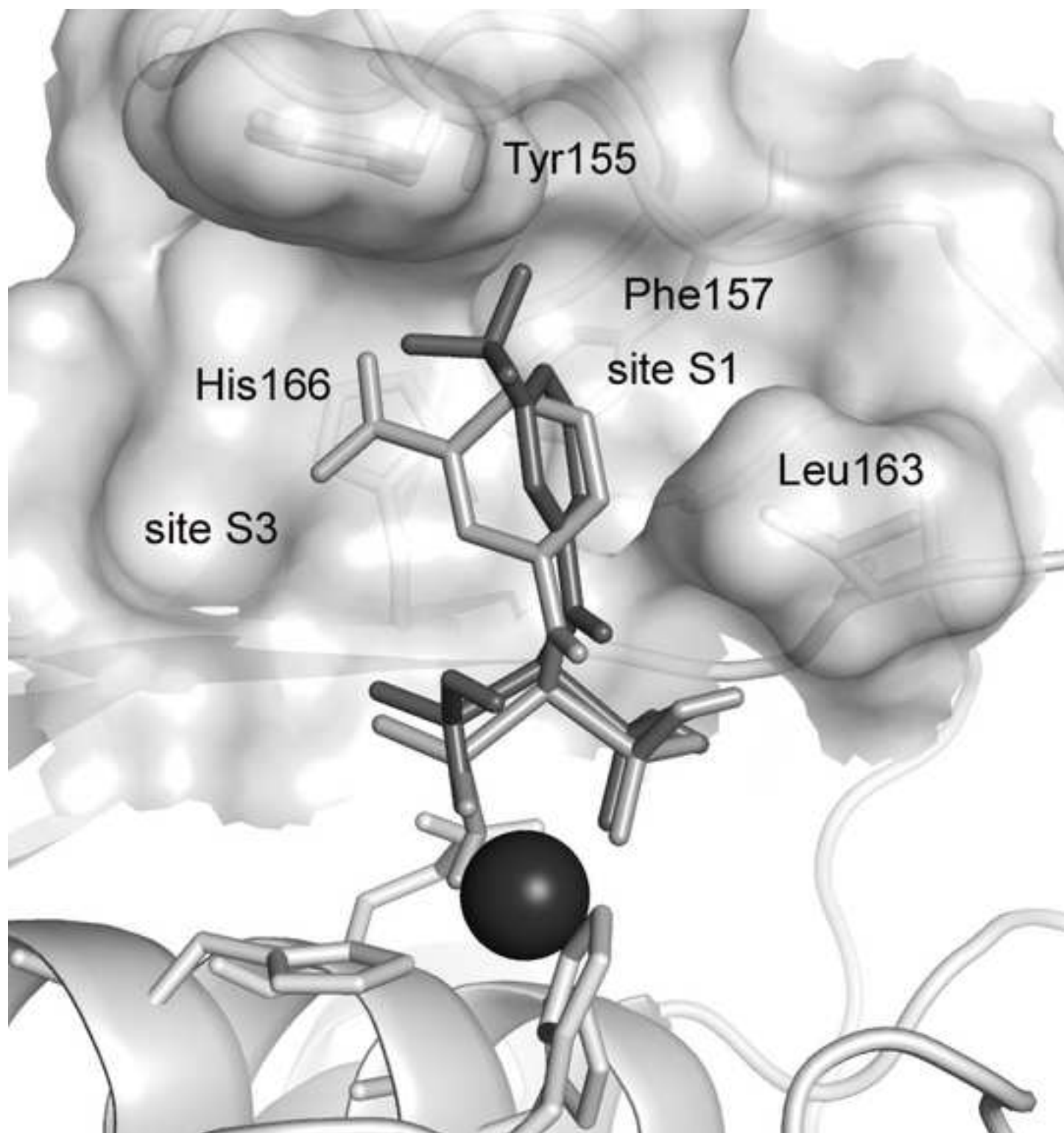


Figure 5 color

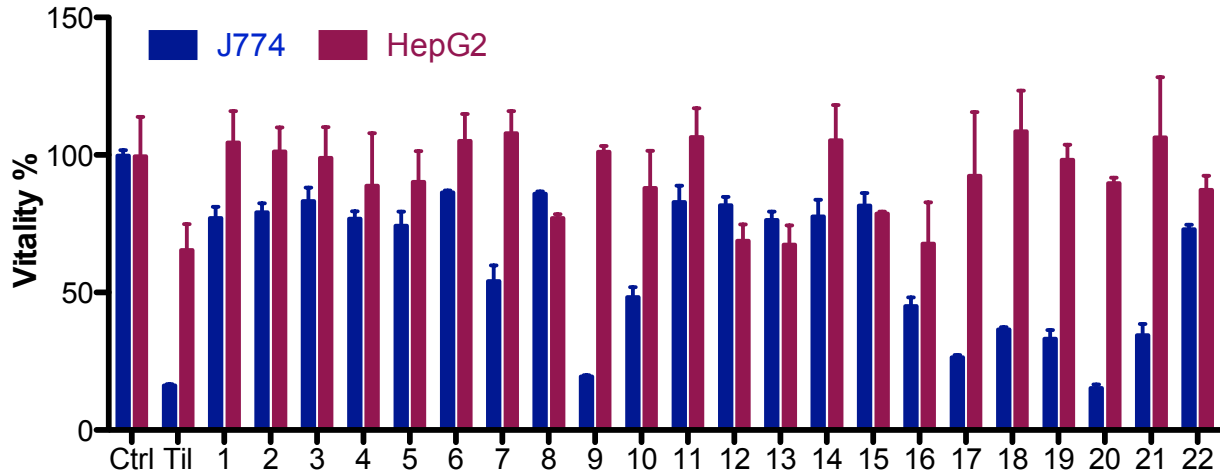
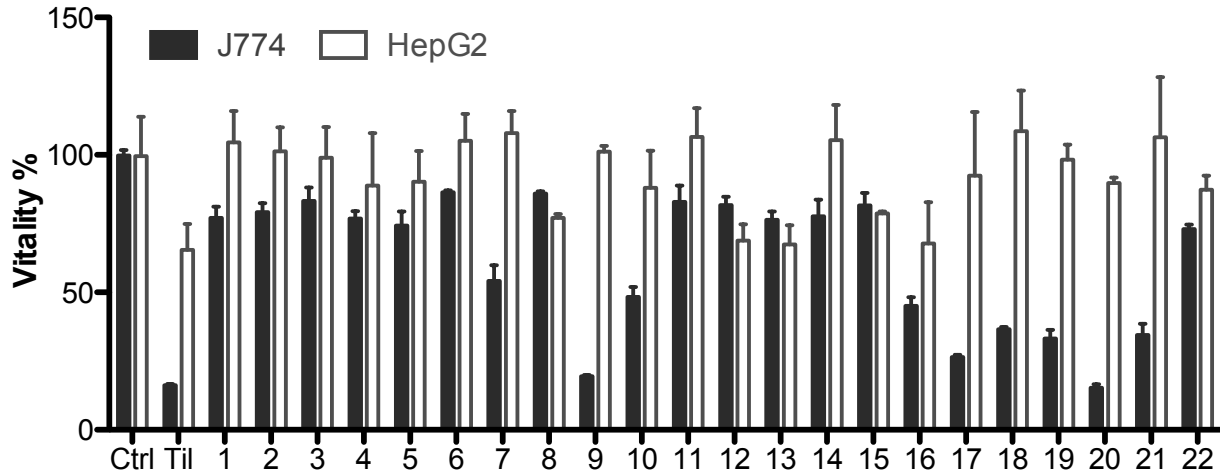
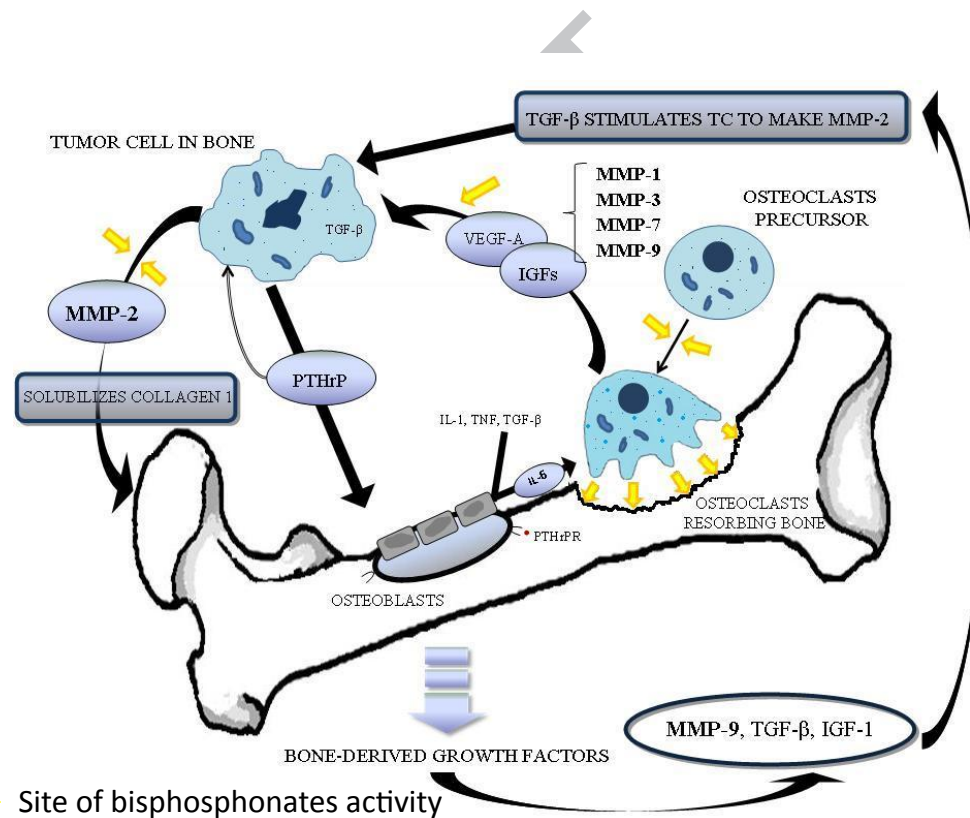
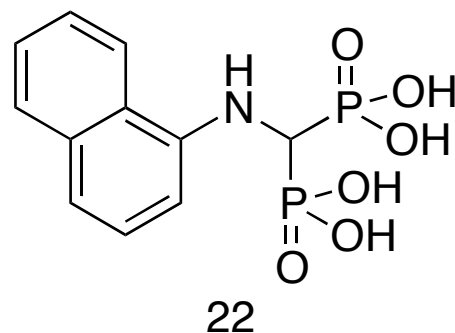
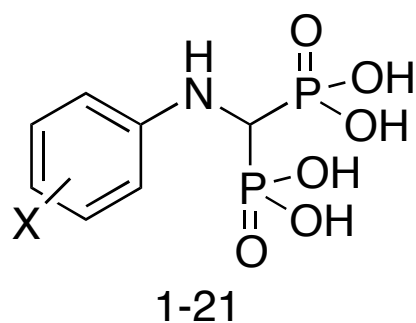


Figure 5 bw



## BISPHOSPHONATES and "VICIOUS CYCLE"



ACCEPTED